CHARACTERIZATION OF CANCER STEM CELLS IN HEPATOCELLULAR CARCINOMA
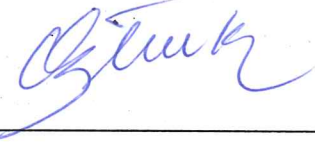
A THESIS SUBMITTED TO

THE DEPARTMENT OF MOLECULAR BIOLOGY AND GENETICS

AND THE GRADUATE SCHOOL OF ENGINEERING AND SCIENCE OF BILKENT UNIVERSITY

IN PARTIAL FULFILLMENT OF THE REQUIREMENTS

FOR THE DEGREE OF

MASTER OF SCIENCE

BY
MERVE DENİZ ABDÜSSELAMOĞLU
JUNE 2014

I certify that I have read this thesis and that in my opinion it is fully adequate, in scope and in quality, as a thesis for the degree of Master of Science.

_____

Prof. Dr. Ihsan Gürsel (Advisor)

_____

Prof. Dr. Mehmet Öztürk (Co-Advisor)

I certify that I have read this thesis and that in my opinion it is fully adequate, in scope and in quality, as a thesis for the degree of Master of Science.
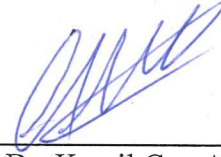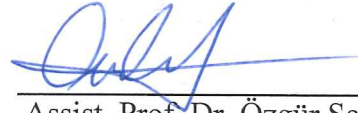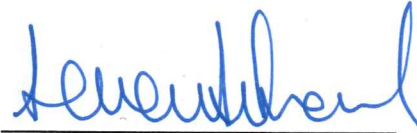
_____

Prof. Dr. Kamil Can Akçalı

I certify that I have read this thesis and that in my opinion it is fully adequate, in scope and in quality, as a thesis for the degree of Master of Science.

_____

Assist. Prof. Dr. Özgür Şahin

Approved for the Graduate School of Engineering and Science

_____

Director of Graduate School of
Engineering and Science
Prof. Dr. Levent Onural

ABSTRACT

CHARACTERIZATION OF CANCER STEM CELLS IN HEPATOCELLULAR CARCINOMA

Merve Deniz Abdüsselamoğlu

M.Sc. in Molecular Biology and Genetics

Supervisor: Prof. Dr. İhsan Gürsel

Co-Supervisor: Prof. Dr. Mehmet Öztürk

June 2014, 96 Pages

Hepatocellular carcinoma (HCC) is the third most common cause of death from cancer worldwide due to the challenges in both its diagnosis and treatment. According to recent studies, HCC tumors, like many other solid tumors are initiated and maintained by a subpopulation of cells called "cancer stem cells (CSCs)" or "tumor-initiating cells (TICs)". HCC stem cells can be identified by the expression of cardinal CD markers such as CD133 (Prominin-1) and epithelial cell adhesion molecule (EpCAM). This study primarily focuses on the investigation of mechanisms involved in the generation of HCC stem cell sub-population using a panel of 15 HCC cell lines. Preliminary data indicates that four cell lines (27%) display $CD133^+$ stem cell populations at frequencies ranging from 8 to 90% when tested by flow cytometry. Among these CD133 positive cell lines, two isogenic cell line with different positivity levels prompted us to focus on two specific cell lines;, i) parental HepG2 cell line and its clone, which was transfected with four copies of hepatitis B virus (HBV), namely ii) HepG2-2215. With tumorigenicity assay induced in atymic nude mice, data revealed that HepG2-2215 that had higher $CD133^+$ ratio, showed higher and rapid tumor formation than parental HepG2 that had much lower $CD133^+$ sub-cellular proportion. Microarray analyses were performed to underpin the mechanisms of in $CD133^+$ cell number variations of these two cell lines. Our initial findings suggested that FGFR signaling pathway might have played a role. To investigate these findings, FGFR signaling pathway was inhibited via potent inhibitor as well as knock down with siRNA. However, preliminary data did not indicate these presumptions and further studies are needed to clarify the relationship between FGFR signaling and CSC formation in HCC. Also, role of suppressive oligodeoxynucleotide (ODN) was studied to see the effects of suppression of DNA-driven immunostimulation. Findings showed that suppressive ODN decreased CD133 levels, which indicates the difference between these two cell lines may arise from the HBV transfection of HepG2-2215 cell line which can produce HBV particles. However, further investigation is needed to understand the relationship between HBV infection and CSC population in HCC.

Keywords: hepatocellular carcinoma, cancer stem cells, CD133, EpCAM, Wnt, TGF-β, FGFR

ÖZET

KARACİĞER KANSERİNDEKİ KANSER KÖK HÜCRELERİNİN BELİRLENMESİ

Merve Deniz Abdüsselamoğlu

Moleküler Biyoloji ve Genetik Yüksek Lisansı

Danışman: Prof. Dr. İhsan Gürsel

Eş Danışman: Prof. Dr. Mehmet Öztürk

Haziran 2014, 96 Sayfa

Hepatosellüler karsinom (HSK) teşhis ve tedavi sürecindeki sıkıntılardan dolayı, dünyada, kansere bağlı ölümlerde ilk üç sırada yer almaktadır. Yapılan son çalışmalara göre, HSK tümörleri, diğer birçok solid tümör gibi, "kanser kök hücreleri (KKH)" ya da " kanser başlatan hücreler (KBH)" olarak adlandırılan hücreler tarafından başlatılır ve tümörün devamlılığı bu hücrelere bağlıdır. HSK kök hücreleri bazı CD markörlerinin ifadesi ile tanınabilir, CD133 (Prominin-1) ve EpCAM de bu markörlerden biridir. Bu çalışma genel olarak, HSK kök hücrelerinin oluşmasında yer alan mekanizmaları, 15 adet HSK hücre hattından oluşan bir panelde incelemeye odaklanmıştır. Ön çalışmalarımız, akış sitometresi deneylerinde, sadece dört hücre hattının (27%), 8-90% olarak değişen oranlarda CD133$^+$ kök hücre topluluğuna sahip olduğunu göstermiştir. Bu CD133 pozitif hücre hatları arasında iki izojenik hücre hattı, farklı pozitivite seviyeleri nedeniyle odaklanmıştır,, i) parental hücre hattı HepG2 ve hepatit B virüsünün (HBV) dört kopyasıyla transfekte edilmiş olan klonu, ii) HepG2-2215. Atymic çıplak farelerde yapılan tümör gelişimini deneyi ile yüksek CD133+ hücre oranına sahip HepG2-2215, daha az CD133+ hücre sayısına sahip HepG2'den daha hızlı ve çabuk tümör oluşumu göstermiştir. Mikro-dizi analizi yapılarak bu hücre hatlarının CD133 $^+$ hücre sayıları farkı altında yatan mekanizmalarını keşfetmek amaçlanmıştır. İlk bulgularımız FGFR sinyal yolağının role sahip olabileceğini düşündürmektedir. Bu bulguları test etmek için FGFR yolağı güçlü bir inhibitör ve siRNA muamelesi ile susturulmuştur. Ancak, ilk veriler bu düşüncelerimizi desteklememiştir. Bu yüzden HSK'da FGRF yolağı ve KKH oluşumu arasındaki ilişkiyi netleştirmek için başka çalışmalara ihtiyaç vardır. Ayrıca, DNA güdümlü immün uyarıcı etkileri susturan, baskılayıcı oligodeoxynucleotide (ODN) rolü DNA çalışılmıştır. Bulgular baskılayıcı ODN muamelesinin CD133 oranlarını düşürdüğünü göstermiş. Sonuçlar, bu iki hücre hattının farklı CD133 positivite oranlarına sahip olmasının sebebinin HepG2-2215 hücre hattının HBV transfekte olup, HBV partikül oluşturmasından dolayı olabileceğine işaret etmiştir. Ancak, HSK'daki KKH nüfusu ile HBV ilişkisini anlamak için daha fazla araştırma gereklidir.

Anahtar sözcükler: hepatosellüler karsinom, kanser kök hücreleri, CD133, EpCAM, TGF-β, FGFR

TO MY FAMILY

.

ACKNOWLEDGEMENTS

TABLE OF CONTENTS

LIST OF TABLES

LIST OF FIGURES

CHAPTER 1

INTRODUCTION

1.1 Hepatocellular Carcinoma

1.1.1 Epidemiology of Hepatocellular Carcinoma

Liver is the largest internal organ in the body and performs many essential roles in digestion, metabolism, immunity and so on [1]. Cancers originate in the liver are called liver cancer. Hepatocellular carcinoma (HCC) is the most common type of primary liver cancers with 80-90% of occurrence in all cases [2]. It is the sixth most commonly occurring cancer and ranked as the third leading cause of cancer-related deaths worldwide [3]. Unfortunately, there are limited treatment options, such as tumor resection, liver transplantation, radiofrequency ablation, and because of high number of patients diagnosed with the disease at advance stage, approximately one third of them are eligible for treatments with 14% overall 5-year survival rate [3, 4]. With age, occurrence rate of HCC increases greatly with the highest prevalence among the population over age of 65 [5]. In addition to the age, sex is a significant factor with a higher occurrence ratio in men.

1.1.2 Aetiologies and Risk Factors of Hepatocellular Carcinoma

Many intrinsic and extrinsic factors interact with each other at molecular level which causes hepatocarcinogenesis [4, 6]. Thus, aetiological factors leading to HCC are complex. Among them, infection with hepatitis B (HBV) and C virus (HCV) contributes to 70% of all cases [7]. Beside these factors, alcohol abuse, aflatoxin contaminated food consumption, immune related factors, metabolic diseases, such as diabetes and obesity, are also other risk factors of HCC [2]. Although all these factors are linked to the incidence of HCC, their efficacy and prevalence depend on the geographical conditions. While HBV infection is the major factor in most Asian and African countries, in Europe and United States, HCV infection is the primary reason for the incidence of HCC [8]. Also, while alcohol abuse is a more common factor in western countries, dietary aflatoxin consumption is more common in South China and Africa [7].

1.1.2.1 Viral Hepatocarcinogenesis

Chronic infection with hepatitis B virus (HBV) or hepatitis C virus (HCV) is the leading etiology for the HCC [9]. And the incidence of HCC parallels with the geographic distribution of these infections. 80-90% of HCC patients were infected with HBV and HCV that promote cirrhosis, initially [10]. HBV and HCV are two unrelated viruses that target liver and reside in hepatocytes [11]. HBV is a small DNA virus, that belongs to hepadnaviridae family and its transmission occurs via contaminated blood products or sexual contact [9]. The virus has 3.2 kb genome consisting of four overlapping open reading frames. Previous studies suggested that chronic HBV infection might increase the risk of HCC up to 100 fold [9, 10]. Integration of HBV DNA can induce chromosomal instability and it allows persistence of the virus [12]. Recent data suggested that HBV is targeting several gene families, such as the telomerase-encoding gene, genes involved in calcium homeostasis, and thus, the expression of some of these target genes are deregulated [12]. Hepatitis B virus X protein (HBx) is 154 amino acid viral protein that has vital

roles in HBV infection, replication and it is also linked to liver carcinogenesis (Fig. 1.1) [9]. The oncogenic potential of HBx can be categorized into four groups; trans-activation or repression of cell survival and proliferation genes, interaction with proteins that have roles in cellular response to oncogenic stress, activation of cell survival signaling pathways and epigenetic changes including DNA methylation, histone modification and microRNA expression [9, 12].
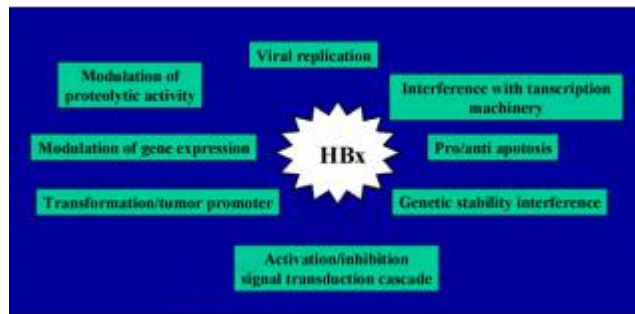
Figure 1.1: Different targets of HBx protein. Adapted from [12].

On the other hand, hepatitis C virus is a positive-sense, enveloped, single-stranded RNA virus, a member of the Hepacivirus genus of the Flaviviridae family [13]. Its genome is 9.6 kb in length and it is associated with a 15- to 20-fold increase in risk for HCC [10]. HCV infection induces several cellular responses, such as ER stress and UPR, autophagy, apoptosis, cell cycle arrest and DNA damage, mitogenic signaling, and PI3K pathway [13].

Thus, HBV and HCV infections together are the strongest risk factors for developing HCC by changing gene expression in liver [11]. These changes includes alterations in DNA methylation, changes in miRNA expression profiles and the constitutive activation of numerous signal transduction pathways [9].

1.1.2.2 Role of Alcohol in Hepatocarcinogenesis

Chronic heavy alcohol consumption is closely associated with hepatocarcinogenesis. Alcohol causes changes in liver structure, especially in hepatocytes [14]. In ethanol

metabolism in liver, ethanol is oxidized by cytochrome P450 2E1 (CYP2E1), generating reactive oxygen species (ROS) [15]. ROS are the most potent agents that can alter DNA methylation patterns in liver [15]. Also, ROS play major role in telomere shortening and favor mutations in oncogenes [2, 14]. Also, chronic alcohol ingestion is associated with enhanced inflammation causing activated monocytes which generates pro-inflammatory cytokines [14]. These cytokines activate Kupffer cells to produce chemokines that have opposite effects on hepatocyte survival [16].

1.1.2.3 Role of Aflatoxin in Hepatocarcinogenesis

Aflatoxins are major mycotoxins that are naturally occurring metabolic byproducts of Aspergillus flavus and Aspergillus parasiticus [17]. Aflatoxins can be found ubiquitously in staple foods, including maize, rice, and ground nuts [18]. Aflatoxin contamination of crops usually occurs in the regions where food drying and storage facilities are not in optimal conditions. They are the most common food-borne risk factor [17]. Exposure to aflatoxin B1 contamination of foods correlates well with the incidence of HCC. The effect of aflatoxin B1 on hepatocarcinogenesis is linked to the mutation caused by aflatoxin exposure in AGG to AGT transversion mutation at codon 249 of the p53 gene [19].

1.1.2.4 Other Factors Inducing Hepatocarcinogenesis

Other than these factors associated with HCC, there are other risk factors implemented to play a role in hepatocarcinogenesis. Diabetes is one of those factors that is thought to promote the onset of HCC with an effect of 2-3 fold increase [20]. Obesity is also a risk factor with diabetes and the reason for this predisposition is possibly caused by insulin resistance that is reduced insulin sensitivity and as a consequence, increased secretion; and accumulation of free fatty acids [21]. Thus, liver fibrosis develops through dysfunctional effects on liver homeostasis.

In addition to diabetes, non-alcoholic steatohepatitis and non-alcoholic fatty liver diseases are likely to promote hepatocarcinogenesis by contributing liver fibrosis and development of cirrhosis [22]. Also, hereditary heamochromatosis, a common genetic disorder, is linked to hepatocarcinogenesis because of excessive iron absorption in hepatocytes [23]. Another inherited genetic disorder which promotes HCC development is alpha1-antitrypsin deficiency. This disease causes antitrypsin polymers formation in liver and as a consequence hepatocyte fatality triggering cirrhosis [24].

1.1.3 Molecular Pathogenesis of Hepatocellular Carcinoma

Molecular pathogenesis of HCC is rather complex including different risk factors and modulations, such as mutations, altered pathways, epigenetic changes, genetic changes and chromosomal aberrations (Fig. 1.2) [2]. Accumulation of these changes leads to neoplastic state in normal, non-cirrhotic and cirrhotic-livers. Actually basis of hepatocarcinogenesis is damaged hepatocytes that start proliferating and regenerating in high frequencies. This increased regeneration activity causes cirrhosis, and then dysplasia, and finally HCC [3].
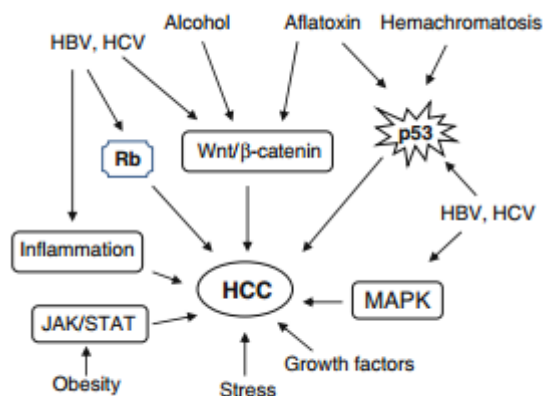
Figure 1.2: *Key signal transduction pathways involved in pathogenesis of HCC. Adapted from [25].*

Transition from normal liver to HCC liver is a multistep process that starts from genetic changes in cirrhotic liver which proceeds into hepatocarcinogenic liver with accumulating changes in the liver [26]. These changes includes mutations that cause genetic alterations, aberrant expression of cellular proteins, overexpression of oncogenes, inhibition of tumor suppressors, and molecules such as microRNAs and various cellular proteins [27]. There are number of critical signaling pathways activated in HCC as well as mutations that inactivates tumor suppressors, such as p53, Rb1, CDKN2A, IGF2R, PTEN; and activates oncogenes like β-catenin, Axin1, PI-3-kinase and K-ras [25]. In the initial steps of HCC, HBV/HCV infections, alcoholic liver cirrhosis, and amplified signaling pathways, such as transforming growth factor alpha and insulin-like growth factor 2, boosts hepatocyte proliferation. These initial steps cause oncogenic activation, instable chromosomes and DNA rearrangements [27]. Further DNA damages induced by oxidative stress and chronic inflammation occur in hepatocytes [25]. Activation of survival and proliferation pathways along with uncontrolled telomerase activity provides unlimited proliferative capacity for these transformed cells [26].

1.1.4 Genetics of Hepatocellular Carcinoma

Initial studies showed that HCC is highly associated with genetic aberrations, chromosomal abnormalities and chromosomal instability. Common alterations include chromosomes 1q, 5, 6p, 7, 8q, 17q and 20 with chromosomal gains whereas 1p, 4q, 6q, 8p, 13q, 16, 17p and 21 are deletion sites [28]. On the other hand, HBV infection often results in integration into host genome which may have cis and trans effects. It is observed that HBV genome integration generally take place within or upstream of TERT (telomerase reverse transcriptase) gene which is the most likely reason of increased telomerase activity [2]. There are a few somatic mutations that are associated with hepatocarcinogenesis. TP53 was the first mutated gene discovered in HCC [29]. TP53, CTNNB1 which encodes for β-catenin and AXIN1 genes display small deletions or point mutation while CDNK2A gene exhibits homozygous deletions and epigenetic silencing [28].

6

1.2 Cancer Stem Cells

In the traditional way, cancer initiation and the progression was explained by the stepwise process of accumulation of genetic and epigenetic changes [30]. This way, cell enters a dedifferentiation state where it gains uncontrollable proliferative ability and tumor formation ability. Thus, this stochastic model suggests that once a random mutation and subsequent clonal selection have taken place, each cell would be equal in terms of forming a new tumor. However, findings in cellular hierarchy and tumor heterogeneity have led to a new model which proposes that only a subpopulation of cells have the ability to self-renew, differentiate and regenerate [31]. This model is the cancer stem cell (CSC) hypothesis which suggests that tumors are organized similarly to normal tissues [32]. Cancer stem cells have the similar capabilities as stem cells, such as self-renewal, giving rise to heterogeneous progeny and dividing in unlimited fashion [33]. CSC hypothesis has been recently validated with various experiments including identification of stem cell marker positivity with hierarchy, serial in vitro clonogenic growth, and in vivo tumorigenicity [33]. These experiments showed that tumor can be initiated from a single cell, cancer stem cell that is also names as tumor initiating cell (TIC) [30]. The first data demonstrating the existence of CSCs was obtained from acute myeloid leukemia (AML) [32]. Studies showed that leukemia stem cells from AML patients are both self-maintaining and can reconstitute all different phenotypes in consistence with CSC model. Meanwhile, similar observations were made in different types of cancers, including breast cancer and glioma [32].

1.2.1 Cancer Stem Cells in HCC and Possible CSC Markers

Like other solid tumors, HCC is thought to contain cancer stem cells (CSCs) as a distinct subpopulation of tumor cells that are capable of tumor relapse and metastasis due to the their abilities to self-renew, differentiate and give rise to a new tumor in local and distant sites [34]. CSCs are identified as tumor initiating properties which inoculations of these cells have continuous cell growth in serial transplantation [35]. These cells are very few in the tumors while the rest of the tumor bulk cannot initiate tumor growth, which are considered to be non-tumorigenic [35].

The first treatment option for HCC is either liver transplantation or surgical resection. However, most HCC patients are at advanced stages which make them inoperable [36]. Other treatment option is chemotherapy but HCC remains largely incurable because of late presentation and tumor recurrence [37]. Also, HCC has chemotherapy-resistant nature with high recurrence rate. The current existing therapies against HCC are generally targeting tumor bulk rather than CSCs [36]. Thus, remaining CSCs lead to re-growth of the tumor. So, isolating and targeting CSCs is very important for better treatment options. A number of molecular markers have been identified for CSCs in HCC, including CD133, epithelial cell adhesion molecule (EpCAM), CD90, CD44, CD13, CD24, OV6, granulin-epithelin precursor (GEP), and Delta-like 1 homolog (DLK1) [36].

Table 1.1: *List of CSC markers in HCC and their possible functional roles. Adapted from [36]*

Marker	Possible Functional Role
CD133	Self-renewal, tumorigenicity, chemo-resistance and invasiveness
EpCAM	Invasiveness, self-renewal, and tumor formation
CD90	-

CD44	Tumor formation, chemo-resistance and metastasis
CD13	Self-renewal, cell proliferation, and tumor formation
CD24	Tumor formation, self-renewal, chemo-resistance, and metastasis
OV6	-
GEP	Self-renewal, chemo-resistance, tumor growth
DLK1	Cell proliferation, self-renewal, tumor formation and tumor growth

CD90 (Thy-1) is 25-37 kDa glycosylphosphatidylinositol-anchored cell surface protein [34]. It has been considered as a marker for various stem cells including CSC in HCC and recent data suggests that there is a positive correlation between CD90 expression with self-renewal, tumorigenicity and metastasis [34, 36]. Meanwhile, CD44 has been associated with various cancer functions, especially metastasis [36]. It is a cell surface glycoprotein and it acts as a receptor for hyaluronic acid and CD44 is a marker in combinations with other CSC markers [34]. CD13 is a newly identified functional marker which can be used to identify dormant liver CSCs resistant to treatments [35]. CD24 is a mucin-like cell surface glycoprotein that has been linked to self-renewal and chemo-resistance [34]. OV6 is a marker for oval cells and it is used widely as hepatic stem cell marker [36]. GEP is a hepatic oncofetal protein that is expressed in fetal liver and associated with recurrence of HCC [36]. Finally, DLK1 is a hepatic stem cell marker that is also expressed in fetal liver.

1.2.2 Prominin 1 (CD133)

CD133 is a member of the prominin family of pentaspan transmembrane glycoprotein that is also known as Prominin 1 (PROM1) [38]. Even though its specific function and ligands are still unknown, CD133 is firstly found hematopoietic stem/progenitor cell marker [38]. CD133 is found in various cancer types, such as brain, prostate, pancreas, colon and liver as CSC marker [34]. Previously, it has been shown that during early liver regeneration, CD133 is up-regulated in liver tissue [36]. Functional studies with CD133$^+$ cell fraction isolated from Huh7 cell line demonstrated that these cells have significantly greater tumorigenicity potential in vitro and in vivo, than CD133$^-$ cells [39]. It has been also found that CD133$^+$ cells have higher colony-forming efficiency and proliferation ability [37, 38]. Further studies revealed that CD133$^+$ cells are more chemo-resistant and radio-resistant because of preferential activation of certain survival pathways, such as AKT/PKB, BCL-2 and MAPK/PI3K pathways [36]. A recent study showed that when compared to its CD133$^-$ counterparts, CD133$^+$ cells showed higher expression of stem cell associated genes (Bmi-1, Notch, Sox2, Oct 4, Nanog, β-catenin, Smo, Nestin, ABCG2 and ABCB1) as well as they have the ability to form undifferentiated tumor spheroids [38].

1.2.3 EpCAM (CD326)

Epithelial cell adhesion molecule EpCAM (murine CD326) is a type I transmembrane glycoprotein with a large extracellular, a single transmembrane and a short intracellular domain [40]. It is known to be expressed in almost all of carcinomas while it is also expressed in embryonic liver, bile duct epithelium and proliferating bile ductules in cirrhotic liver [34]. Recent findings suggest a role for EpCAM as an early biomarker for HCC because of its high expression in premalignant hepatic tissues [34]. EpCAM$^+$ HCC cells have been shown to possess ability of self-renewal, differentiate and initiate tumors [36]. EpCAM plays a role in

cell proliferation, migration and mitogenic signal transduction. EpCAM also has been shown that it is a direct transcriptional target for Wnt/β-catenin signaling pathway [39, 41]. Further studies with microarray analysis with primary HCC tissue demonstrated that EpCAM+ HCC was associated with gene signature and the molecular pathway of hepatic progenitor cells. Meanwhile EpCAM- HCC cells were linked to mature hepatocytes [37].

1.3 Signaling Pathways in CSCs

During hepatocarcinogenesis, two main pathogenic mechanisms are observed. First one is cirrhosis associated with hepatic regeneration after tissue damage caused by several reasons, such as exposure to toxins, viral infections or metabolic influences, while the other mechanism is the occurrence of mutations in single or multiple oncogene or tumor suppressors [42]. In HCC, many major signaling pathways implicated, including Wnt/β-catenin, PI3K/AKT1/mTOR, RAF/MKK1/MAPK3, IGF-1, HGF/c-MET and TGF-β [42]. Interestingly, many of these pathways are known to be involved in stem cell maintenance self-renewal and pluripotency, such as MET, Hedgehog, MYC, p53, EGF, Wnt/β-catenin, TGF-β, etc [41]. Many of these signaling pathways are also found in CSCs which also suggest that these pathways should be investigated in HCC CSCs.

1.3.1 Wnt Pathway

The Wnt pathway is a highly conserved signaling pathway whose first member was identified in fruit fly [43]. The Wnt family consists of 19 Wnt ligands identified and the intracellular signaling is maintained via two different pathways; "canonical" and "non-canonical" [43]. The canonical Wnt pathway is activated by the binding of Wnt ligands to the transmembrane Frizzled receptor and its co-receptor LRP 5 or 6, and then, scaffolding protein Dishevelled (Dvl) is recruited. This stabilizes destruction complex composed of APC, AXIN1, GSK3β and CSNK1A1 which normally

phosphorylates β-catenin leading to its ubiquitination and degradation [32, 44]. Thus, stabilized b-catenin translocated to nucleus in order to regulate transcription with TCF/LEF complex [44]. Wnt signaling plays an important role in embryonic development, growth, survival, regeneration, and self-renewal as well as in tumor development. It has been shown that several Wnt ligands were expressed by various liver cells, and Wnt/β-catenin pathway plays a crucial role in prenatal development, hepatic fate specification of stem cells and liver organogenesis [43]. Aberrant activation of Wnt pathway is a factor participating HCC development [45]. Disrupted Wnt pathway by mutational or non-mutational events is observed in one third of all HCCs [46]. Activation of canonical Wnt pathway drives tumor formation in liver stem cells and the higher β-catenin expression was found in HCC than non-tumor tissues [47]. The Wnt pathway also plays a crucial role in regulating stem/progenitor cell expansion as well as the determination of self-renewal or differentiation [48]. The elevated expression of Wnt and its downstream mediators were found in CD133^{+} or EpCAM^{+} HCC cells which suggest that Wnt/β-catenin signaling pathway is implicated in HCC CSCs [41].

1.3.2 Transforming Growth Factor (TGF)-β Pathway

Transforming growth factor (TGF)-β superfamily consists of TGF-βs, activins, inhibins, Nodal, bone morphogenic proteins (BMPs) and anti-Müllerian hormone (AMH) and regulates many cellular functions, including cell growth, differentiation, apoptosis, extracellular matrix (ECM) production, immunity and embryonic development [49]. Canonical TGF-β pathway is activated via binding of TGF-β ligand to the heteromeric receptor complex which phosphorylates receptor activated SMAD (R-SMAD) proteins. Activated R-SMADs together with SMAD4 translocates to nucleus to act as transcription factor complex [50]. TGF-β signaling pathway has a role in cell cycle regulation, the immune system and apoptosis. In HCC, it plays a crucial role in inhibiting oncogenesis at an early stage by inducing apoptosis and activates autophagy in certain HCCs in order to suppress tumor formation [47]. On the other hand, dysregulation of TGF-β signaling is associated with

hepatocarcinogenesis [51]. TGF-β signaling pathway is involved in self-renewal, differentiation and carcinogenesis [52]. Also, TGF-β co-operates with oncogenic RAS to activate nuclear β-catenin, which causes neoplastic hepatocyte differentiation into immature progenitor cells and facilitates HCC recurrence [47]. Finally, TGF-β plays a crucial role in maintenance of CSCs in HCC and it has been shown that lack of responsiveness to TGF-β led to the generation of CSCs [41].

1.3.3 Fibroblast Growth Factor Receptor (FGFR) Signaling Pathway

Fibroblast growth factor (FGF) superfamily consists of structurally related polypeptides where most of them function through fibroblast growth factor receptors (FGFRs) [53]. In humans, FGFs are encoded by 22 genes which are divided into 7 subfamilies. FGFRs are transmembrane tyrosine kinase receptors and are activated by binding of FGF ligands [54]. Binding of FGFs to FGFRs activates downstream signaling, enabling trans-phosphorylation of tyrosines in the intracellular part of receptor and these phophorylated tyrosine residues act as docking sites for various adaptor proteins which promotes activation of different signaling pathways, including Ras/Raf/MAPK, PI3K signaling pathway [54]. Thus, FGFR signaling pathway promotes cell growth, epithelial-mesenchyme transition and survival [56]. FGFR2 isoform b (FGFR2-IIIb) is highly expressed in hepatocytes and plays a crucial role in liver homeostasis and regeneration [55]. Studies showed that alterations in FGFR signaling pathway could lead to cancer [54]. Some of the FGF ligands are up-regulated in HCC and have been shown to initiate autocrine growth stimulation, cell survival and neo-angiogenesis [57]. Moreover, some FGF ligands were associated with more aggressive behavior of malignant hepatocytes and this might involve Wnt signaling pathway as well [58].

1.4 Suppressive Oligodeoxynucleotides (ODNs)

Normally, DNA is isolated via nuclear or mitochondrial membrane in eukaryotes, or by the cell wall in bacteria or the envelope in viruses. However, following a microbial infection or tissue damage, DNA can be released [59]. In this case, due to its high unmethylated CpG motif frequency, bacterial DNA can be recognized as "non-self" via TLR9 and trigger an innate immunity response. This CpG-driven-immune activation can exacerbate inflammatory tissue damage, or increasing sensitivity to autoimmune diseases or toxic shock [60].

On the other hand, some immune responses are designed to protect the host. Previous studies suggested that some antagonistic elements are present in the host DNA possibly to suppress DNA-driven immunostimulation [61]. Thus, these neutralizing or suppressive motifs can block CpG-mediated immune system selectively [62]. These suppressive motifs are rich in poly-G or –GC sequences, and surprisingly, optimal motifs are identical to telomere motifs (with a repeat of TTAGGG) [63]. It has been shown that suppressive oligodeoxynucleotide (ODN) (A151) inhibits the production of several pro-inflammatory cytokines and chemokines induced by bacteria [63]. So, in different autoimmune and inflammatory diseases, the effects of suppressive ODN (A151) have been studied. Over the last few years, suppressive ODN (A151) has been studied in cancer types, especially in cancers that inflammation plays a crucial role. It has been shown that suppressive ODN can be used in inflammation associated oncogenesis [64]. This observation was supported with other studies showing that suppressive ODN can improve the anti-proliferative effects of anticancer drugs [65]. Meanwhile another study showed that suppressive ODNs actually repress fibrosis and down-regulates stemness (Aydin, M. et al., unpublished data).

1.4 Aim of the Study

Like other solid tumors, HCC has been shown to possess a small subpopulation of cancer stem cells that are responsible from initiation, maintenance and recurrence of tumor [36]. These cells also show the ability to self-renew, give rise to different phenotypes of cells which accomplish tumor heterogeneity and chemo- or radio-resistance. After the initial treatment, these CSCs are the ones who resisted the therapy and provided the re-growth of tumor. Thus, the idea of targeting these cells might be a better therapeutic approach along with traditional treatment methods in order to achieve better cure rate for the disease.

However, targeting these cells requires more knowledge on the characterization of cancer stem cells in HCC. Molecular mechanisms underlying the process of these transformed cells into cancer stem cells might be the direct targets of future treatment methods to reverse this transition or at least it might provide opportunity to make cancer stem cells more vulnerable to the current treatments. The outcomes of this study are expected to make contributions to the field of new therapeutic approaches for HCC.

CHAPTER 2

MATERIALS AND METHODS

2.1 MATERIALS

2.1.1 General Laboratory Reagents

Most of the reagents used in this research including Bradford reagent, haematoxylin, ethanol and methanol were purchased from Sigma-Aldrich (St. Louis, MO, USA) and Merck (Darmstadt, Germany). ECL+ blot detection kit and western blot membranes were purchased from Amersham Pharmacia Biotech Company. DMSO and Ponceau S were purchased from Applied Biochemia (Darmstadt, Germany). Fluorescent mounting medium was from Dako (Denmark). Nucleospin RNA II total RNA isolation kit and DNase I was from Macherey-Nagel (Duren, Germany). Collagenase type I was purchased from Sigma-Aldrich (C0130-500MG, St. Louis, MO, USA) and Fixative Medium A was bought from Invitrogen (GAS003, Carlsbad, CA, USA).

2.1.2 Cell Culture Materials and Reagents

Dulbecco's modified Eagle's medium (DMEM) and Roswell Park Memorial Institute (RPMI) 1640 medium and OptiMEM were purchased from GIBCO (Invitrogen, Carlsbad, CA, USA). Penicillin/streptomycin antibiotics, L-glutamine, trypsin-EDTA, fetal calf serum (FCS) was also from GIBCO. All plastic materials used in

cell culture, such as tissue culture flasks, petri dishes, plates, cryovials were purchased from Corning Life Sciences Inc. (USA). Serological pipettes were from Costar Corporation (Cambridge, UK). RNAi Max was purchased from Invitrogen.

2.1.3 Spectrophotometry

Bradford based protein concentration measurements were done using spectrophotometer Beckman Du640 from Beckman Instruments Inc. (CA, USA).

2.1.4 Antibodies

In this study, there are numerous primary and secondary antibodies from various sources. Antibodies, their catalog numbers, and working dilutions are given below in Table 2.1.

Table 2.1: *Antibody list, catalog numbers and working dilutions*

Antibody	Company and catalog number	Western Blot Dilution	Immunostaining Working Dilution
Calnexin	Sigma, C4731	1:5000	-
α-tubulin	Calbiochem, CP06	1:5000	-
Anti-mouse-HRP	Sigma, A0168	1:5000	-

Anti-rabbit-HRP	Sigma, 6154	1:5000	-
Anti-goat-HRP	Abcam, ab6741	1:5000	-
Anti-mouse/rabbit-Alexa Fluor 488	Invitrogen, A11034	-	1:750 (IF)
Anti-mouse/rabbit-Alexa Fluor 568	Invitrogen, A11034	-	1:750 (IF)
β-actin	Sigma, A5441	1:10000	-
P-FGFR	R&D Systems	8μg/mL	-
Sox9	Millipore, AB5535	1:1000	1:1500 (IF)
HNF4α	Santa Cruz Biotechnologies, sc-6556	1:300	1:150 (IF)
Bek antibody	Santa Cruz Biotechnologies, sc-6930	-	1:30 (Flow Cytometry)
CD133 pure	Miltenyi, 130-090-422	-	1:100 (IP, IF)
CD133-APC	Miltenyi, 130-090-826	-	1:30 (Flow Cytometry)
EpCAM-FITC	Miltenyi, 130-080-301	-	1:30 (Flow Cytometry)

Anti-acetylated-α-tubulin	Abcam, ab24610	1:2000	-
Anti-Histone H3	Abcam, ab1791	1:5000	-
Anti-acetyl-H4	Millipore, 06-866	1:5000	-

2.1.4.1 Antibody Conjugation Kit

Lightning-Link Atto488 Conjugation kit (733-0010) was purchased from Innova Biosciences.

2.1.5. Immunoperoxidase Staining Reagent

In immunoperoxidase staining experiments; DAKO EnVision+ System was used, DAKO (Glostrup, Denmark).

2.1.6. Suppressive Oligodeoxynucleotide and Control Oligodeoxynucleotide

All oligodeoxynucleotide (ODN) types used in this study listed in Table 2.2 with their working concentrations.

Table 2.2: *List of ODNs used in this study.*

Name	Concentration
A151 (suppressive ODN)	0.5 - 3μM

D35 flip	0.5 - 3μM

Oligodeoxynucleotides (ODN) sequences given below were purchased from either Alpha DNA, (Canada) or NIH or USFDA CBER Core Facility (USA), or synthesized in the Biotherapeutic ODN Research Lab. Facility on a MerMade6 Oligonucleotide synthesizer machine:

A151   5' TTAGGGTTAGGGTTAGGGTTAGGG 3'

D35 flip-   5' ggTGCATGCATGCAGGGGgg 3'

2.2 SOLUTIONS AND MEDIA

2.2.1 General Solutions

10X Phosphate Buffered Saline (PBS)   80g NaCL, 2g KCl, 14.4g Na_2HPO_4, 2.4g KH_2PO_4 in 1 litre ddH_2O

Working dilution is 1X.

10X Tris buffered saline (TBS)   12.9g Trisma base, 87.76g NaCL, in 1 litre ddH_2O, pH is adjusted to 8.0

Working dilution is 1X.

2.2.2 Tissue Culture Solutions

DMEM/RPMI media	Complete medium contains 10% Fetal calf serum, 1% penicillin/streptomycin, 1% non-essential amino acids, stored at 4 ℃
Serum free DMEM/RPMI media	0.01% Fetal calf serum, 1% penicillin/streptomycin, 1% non-essential amino acids, 1mM Na_2SeO_3, stored at 4 ℃
10X Phosphate buffered saline (PBS)	80g NaCL, 2g KCl, 14.4g Na_2HPO_4, 2.4g KH_2PO_4 in 1 litre ddH_2O Working dilution is 1X, stored at 4 ℃

2.2.2.1 Preparation of Wnt-3a and WIF1

Reconstitute Recombinant Human Wnt-3a (R&D Systems, 5036-WN/CF) at 200μg/mL in sterile 1X PBS. Working concentration is 250ng/mL. Reconstitute Recombinant Human WIF-1 (R&D Systems, 1341-WF/CF) at 200μg/mL in sterile 1X PBS. Working concentration is 250ng/mL.

2.2.2.2 Preparation of TGF-β1 and anti-TGFβ1 antibody

Reconstitute TGF-β1 (R&D Systems, 240-B) at concentration of no more than 10μg/mL in filter-sterilized 4mM HCl containing 1mg/mL bovine serum albumin to ensure complete recovery from glass surfaces. Working concentration is 5ng/mL. Reconstitute TGF-b1 antibody (monoclonal mouse IgG1, R&D Systems, Mab240) at 0.5mg/mL in sterile 1X PBS. Working concentration is 5μg/mL.

2.2.2.3 Preparation of SU5402

Reconstitute SU5402 (Santa Cruz Biotechnologies, sc-204308) at 1mM in sterile DMSO. Working concentrations between 2μM to 50μM were tired.

2.2.3 Immunoperoxidase Solutions

Acetone: methanol fixation reagent	Acetone and methanol were mixed in 1:1 ratio and stored at -20 ℃
3% H_2O_2 solution	Dilute 30% H_2O_2 with methanol and ddH_2O. (For example, 3mL H_2O_2, 10mL methanol, and 17mL ddH_2O)
Immunoperoxidase blocking solution	10% FCS in 0.3% TritonX-100 in 1X PBS
Washing solution	0.3% TritonX-100 in 1X PBS
Antibody dissolved in	10% FCS in 0.3% TritonX-100 in 1X PBS
DAB solution	DAB chromogen and its substrate from Dako were used according to the manufacturer's protocol

2.2.4 Immunofluorescence Staining Solutions

4% Formaldehyde	It is prepared dissolving 50mL 40%

formaldehyde in 450ml ddH$_2$O.

4% Paraformaldehyde	Dissolve 4g paraformaldehyde in 100mL ddH$_2$O, heat at 130℃ for 1 hour, cool before use
Immunofluorescence blocking solution	10% FCS in 0.2% PBS-Tween 20
Washing solution	0.2% PBS-Tween 20
Antibody dissolved in	10% FCS in 0.2% PBS-Tween 20
DAPI (4',6-diamino-2-phenylindole)	0.1-1µg/ml working solution in PBS or ddH$_2$O

2.2.5 Sodium Deodecyl Sulphate (SDS) – Polyacrylamide Gel Electrophoresis (PAGE) and Immunoblotting Solutions

In this study, tris-glycine gels and buffers were prepared manually according to a conventional protocol in our lab. To prepare 5% stacking gel, 30% acrylamide mix, 1.0M Tris-HCl pH 6.8, 10% SDS, 10% ammonium persulphate and ddH$_2$O were mixed in appropriate amounts. For the resolving gels, same ingredients were mixed depending on the gel concentration changing between 8% to 12%, with the exception of using 1.5M Tris-HCl pH 8.8 this time. Wet transfers were done to either PVDF membrane or nitrocellulose. 10X transfer buffer for wet transfer, 5X sample loading buffer and 10X denaturing reagent (500mM DTT) were also purchased from Invitrogen.

10X SDS Running buffer	144g glycine and 30g Tris were dissolved in ddH$_2$O, 50mL 10% SDS was added, and the

volume was completed to 1L. Working solution is 1X

10X Transfer buffer	72g glycine and 58g Tris were dissolved in ddH$_2$O, 2mL 10% SDS was added, and the volume was completed to 1L. Working solution is 1X containing 10-20% Methanol depending on protein size.
Blocking solution	5% (w/v) non-fat dry milk was dissolved in 0.2% TBS-Tween 20, or 5% (w/v) bovine serum albumin (BSA) was dissolved in 0.2% TBS-Tween 20
10X Tris buffered saline (TBS)	12.9g Trisma base, 87.76g NaCl in 1L of ddH$_2$O, working dilution is 1X and pH 8
TBS-Tween 20	0.2% Tween 20 in 1X TBS
Ponceau S	0.1% (w/v) Ponceau S and 5% (v/v) acetic acid was dissolved in 0.2 % TBS-Tween 20
Coomassie brilliant blue solution	100mg coomassie brilliant blue G-250, 50ml 95% ethanol, 100ml 85% phosphoric acid. Filtered using whatman paper
NP-40 lysis buffer	50mM Tris HCl, 150mM NaCl, 1% NP-40, 0.1% SDS, 1X protease inhibitor cocktail

2.2.6 Flow Cytometry Analysis Solutions

Fixative Medium A	Fix cells, Invitrogen, GAS003
Antibody dissolved in	PBS-BSA-NaAzide, prepare by adding 500mg NaAzide and 10g BSA in 1L 1X PBS, store at +4℃
10X Phosphate Buffered Saline (PBS)	80g NaCL, 2g KCl, 14.4g Na_2HPO_4, 2.4g KH_2PO_4 in 1L ddH$_2$O Working dilution is 1X.

2.2.7 Single Cell Isolation from Xenograft Tumor Solutions

Dissociation Buffer	Prepare DMEM containing 10% FCS and dissolve 125U/mL Collagenase type I and 150U/mL DNase I in it, prepare fresh

2.3 METHODS

2.3.1 Tissue Culture Methods

2.3.1.1 Cell lines and growth condition of cells

Hepatocellular carcinoma cell lines used in this study were cultured in either DMEM or RPMI media supplemented with 10% fetal calf serum (FCS), 1% non-essential amino acids, 100mg/mL penicillin/streptomycin and 1% L-glutamine at 37^0C and 5% CO_2. Cell lines Huh-7, Hep40, HepG2, HepG2-2215, Hep3B, Hep3B-TR, PLC, Mahlavu, Focus, FLC4, SK-HEP-1 cell lines were cultured in complete DMEM medium. Other HCC cell lines Snu-182, Snu-387, Snu-398, Snu-423, Snu-449, and Snu-475 were cultured in complete RPMI medium. Cells were passaged into new dishes or plates before they reached high confluency in the dish.

2.3.1.2 Passaging the Cells

To passage cells, firstly, the medium was aspirated using sterile glass pipettes and the cells were washed at least once with 1X PBS. Then, trypsin-EDTA was added in the plate or flask. The amount of trypsin-EDTA was between 0,5- 2ml, depending on the surface area of the flask or plate. Trypsinized cells were kept in the incubator for 1-2 minutes for the detachment of the cells from the surface. Then, detached cells were collected in a complete medium using serological pipettes. Cells were mixed by pipetting up and down. Desired portion of the collected cells were reseeded on plates or flasks depending on the requirements.

2.3.1.3 Thawing the Cells

One vial of stock cryovial of interest was taken either from nitrogen tank stocks or from – 80 °C freezer stocks and put on ice immediately. The vial was put in the 37 °C water bath in order to have cell suspension quickly. Cells were resuspended by pipetting up and down gently, and transferred into a 15mL falcon tube with several milliliters of complete medium. Cells were then centrifuged for 4 minutes at 1500 rpm. Supernatant containing DMSO was removed and cell pellet was resuspended in a complete medium and transferred into plate or flask. Flasks and plates were chosen depending on the amount of pellet, smaller flask or dish for less amount of cell pellet. Cells were distributed in the flask or dish evenly by moving the flask or the dish back-forth and right-left. Cells were kept in incubators, at 37 C and 5% carbon dioxide conditions. The day after, cells were washed and unattached cells were removed and the mediums were refreshed.

2.3.1.4 Cryopreservation of the Cells

Cell stocks were prepared from the cell in culture with around 60-75% confluency. These cells were washed with 1X PBS and trypsinized with appropriate amount of trypsin-EDTA. Then, cells were collected with complete medium afterwards in 15mL falcon tube. Cells were centrifuged for 4 minutes at 1500 rpm. Thereafter, freezing medium, containing 10% DMSO and 20% FCS in complete medium, was added for resuspending the cells and then, to transfer cell suspension into cryotubes. Cryotubes were first kept at -20 °C for about 1 hour. Afterwards, they were stored at – 80 °C overnight and transferred into nitrogen tanks.

2.3.1.5 Treatment of the Cells

Firstly, cells were seeded in appropriate dishes, flasks or plates according to the experiment type. One day after the seeding, the mediums were removed and cells were washed either with 1X PBS or serum free media which contains only 0.01% FCS depending on the experiment type. Some treatments were done in complete DMEM or RPMI mediums. Some treatments are done in serum free medium containing 1mM Na_2SeO_3. And one treatment way is to apply serum free medium containing 1mM Na_2SeO_3 to achieve serum starvation in the environment. Treatment mediums containing chemicals, such as Wnt3a or WIF1, etc. was prepared freshly. For the control samples, complete mediums containing same amount of solvents were prepared, such as water or DMSO. For ODN and microbial byproducts treatment, cells were seeded on the first day and on the second day, medium containing these elements were added onto the cells. Cells were incubated as long as desired.

2.2.1.6 Transient Transfection of Cells with RNAi Max

First of all, siRNA amount to be used should be decided. For this, a trial can take place to find the appropriate amount ranging from 10 to 100nM. To transfect the cells, HepG2 and HepG2-2215 cell lines can be reverse transfected where cells will be seeded while transfection was performed. To do so, in the plate (6-well plate), appropriate amount of siRNA is mixed with appropriate amount of RNAi Max in OptiMEM medium without any serum and media. Then, this should be incubated for 10-20 minutes. After that, trypsinized and counted cells were seeded onto the plate. Cell number should be about 30-40% confluency. After cell seeding, plate should be mixed very well. Depending on your purpose, cells can be examined in 24-72 hours.

2.3.2 Total RNA Extraction from Cultured Cells

For RNA extraction from the cultured cells, first of all, cells were collected by adding trypsin-EDTA and growth medium. Then, cells were centrifuged and the pellets were used for RNA extraction using NucleoSpin RNA II Kit (MN Macherey-Nagel, Duren, Germany) according to the manufacturer's protocol.

2.3.3 Immunoperoxidase Staining Assay

For immunoperoxidae staining, first of all, cells or tissues were fixed with 1:1 acetone:methanol solution for 10 minutes at -20°C. After fixation, cells or tissues were washed with 1X PBS. To stop endogenous peroxidase activity, they were treated with 3%H2O2 for 10 minutes for cells and 30 minutes for tissues. Then, cells or tissues were blocked with 10% fetal calf serum and 0.3% TritonX-100 in PBS. They were incubated with primary antibodies for 1 hour in PBS containing 10% fetal calf serum and 0.3% TritonX-100 solution. After washing with 1X PBS containing 0.3% TritonX-100, cells or tissues were incubated for 1 hour with Cytomation Envision+Dual link system-HRP (Dako), and eventually the staining was performed with DAB detection solution (Dako). Cover slips were then rinsed with distilled water and counterstained with haematoxylin (Sigma) for 3-4 min, mounted on glass microscopic slides using 90% (v/v) glycerol and examined under light microscope.

2.3.4 Immunofluorescence Staining Assay

For immunofluorescence staining, first of all, cells were fixed with 4% formaldehyde for 10 minutes at room temperature, or tissues were fixed with 4% paraformaldehyde for 30 minutes at room temperature. After fixation, cell permeabilization was done using 0.5% saponin, 0.3% TritonX-100 in 1X PBS solution for 5 minutes, three times at room temperature. This step was not needed in immunofluorescence protocol for

tissues. Permeabilized cells or tissues were blocked with 10% fetal calf serum (FCS), and 0.3% TritonX-100 in 1X PBS for 1 hour at room temperature. After blocking, primary antibody incubation was done using a specific antibody prepared in 10% fetal calf serum and 0.3% TritonX-100 in 1X PBS for 1 hour at room temperature. Primary antibodies were removed and cells were washed with PBS-0.3% TritonX-100. Then, secondary fluorescent antibodies, anti-rabbit or anti-mouse or anti-goat Alexa Fluor 488 or Alexa Fluor 568 were used for the detection of the primary antibody. After secondary antibody incubation, cells or tissues were counter stained with DAPI (1:10000 dilution in ddH2O) for 1 minute. Finally, cover slips were mounted on slides using fluorescent mounting medium and visualized and photographed under fluorescence microscope.

2.3.6 Western Blotting

After quantification of the protein concentrations of the samples, equal amounts of proteins were used to prepare loading mixtures. 25 to 50μg of proteins were loaded into the gel according to the type of experiment. Loading samples were prepared by adding 5X Loading buffer, 20X denaturing agent (or 2M DTT), and ddH2O up to the final volume of 20 or 30μl per well. Then, prepared loading mixtures were heated at 100 °C for 10 minutes and chill on ice before loading into the gel.

In this study, gel concentrations and type of running buffers were chosen mainly according to size of the protein of interest. 8%, 10%, and 12% tris-glycine gels were the type of gels used. After running, proteins were transferred onto Amersham HyBond ECL nitrocellulose or PVDF membranes with wet transfer protocol. Transfer buffer was prepared 1X (from 10X stock) with 10% or 20% methanol in ddH$_2$O. Before preparation of wet transfer sandwich, all of the materials were soaked into transfer buffer, and especially PVDF membranes were extra activated in absolute methanol before soaked into transfer buffer. Transfer was done for 90-120 minutes (longer for proteins with very high kDa) with 100 V voltage applied. During the transfer, western blot tank was either kept in cold room or covered with ice.

When the transfer was completed, the efficiency of transfer was tested by putting membrane into Ponceau S solution for 30 seconds. Then, Ponceau S solution was removed by washing membrane in ddH2O for a few minutes. Membranes were blocked with 5% non fat dry milk, or 5% BSA in 0.2% TBS-Tween for 1 hour. Short time blockings were done at room temperature, whereas over night blockings at +4 °C. After blocking, primary antibodies were prepared in non fat dry milk solution or BSA solutions and incubated for 1-2 hour(s) at room temperature or over night at +4°C. After primary antibody incubation, membranes were washed with 0.2% TBS-T five times for 5, 5, 10, 5, 5 minutes at room temperature. Then, horseradish peroxidase conjugated secondary antibodies; anti-mouse, anti-rabbit or anti-goat, were used as secondary antibodies according to the type of primary antibody used. Secondary antibody incubation was performed at room temperature for 1 hour. After this incubation, membranes were again washed five times for 5, 5, 10, 5, 5 minutes at room temperature on a shaker. Then, detections were done using chemiluminescent detection kit, ECL+ (Amersham, UK) according to the manufacturer's protocols. Finally, X-ray films were exposed to the emitted chemiluminescent light from the reaction of horseradish peroxidase and developed in X-ray developer. Time of exposure was chosen depending on the detection reagent and the specific antibody used against the protein of interest.

2.3.7 Flow Cytometry Analysis

Firstly, treated or untreated cells were trypsinized and they were collected with appropriate amount of medium in 15mL falcon tubes. Cells were washed twice with 1X PBS and they were centrifuged at 1600 rpm for 5 minutes. Then, fixative reagent A was added to cell pellets while vortexing samples for 10 seconds. They were incubated at room temperature for 15 minutes. Cells were washed with 1X PBS containing BSA-NaAzide. Then, cells were incubated with primary antibodies that are conjugated with fluorescent dyes, which are diluted in PBS-BSA-NaAzide for 10 minutes at +4°C. Then, cells were washed twice with PBS-BSA-NaAzide. Finally

cells were resuspended in 1X PBS and analyzed using BD CSampler. Antibody positivity was assessed depending on the fluorescent intensity of the samples.

2.3.8 Antibody Conjugation

Antibody to be labeled with Atto488, should be 100-200µg in 40-100µL. For each 10µL of antibody to be labeled, 1-2µL of LL-Modifier reagent should be added, and mixed gently. This solution should be added directly onto the Lightning-Link mix vial and lyophilized mix should be resuspended with antibody solution. The mix should stand 3 hours to overnight incubation at room temperature. After incubation, 1µL of LL-quencher FD reagent should be added to mix for each 10µL of antibody. The conjugate can be used after 30 minutes. The conjugate will be Alexa488 labeled and it should be stored at 4°C.

2.3.9 RNA Sample Preparation and Hybridization to Chip

Total RNA isolation from triplicate samples of HepG2 and HepG2-2215 cell lines treated with 3 days of serum starvation was performed with Nucleospin RNA kit (MN, Düren, Germany) according to the manufacturer's protocol. RNA quality was checked using Agilent Bioanalyzer 2100 kit and software (Agilent Technologies, Santa Clara, CA, USA) according to the manufacturer's protocol. RNA isolates were hybridized to Affymetrix HG-U133_Plus2 chips, applying Affymetrix 3' IVT hybridization protocol in Bilkent University Bilgen Affymetrix Center for microarray analysis.

2.3.10 Data Analysis of Microarray Samples

Microarray data normalization and class comparison analyzes was performed using BRB-Array Tools Version 4.2.1 [66]. Triplicate HEPG2 and HEPG2-2215 samples,

which passed the Affymetrix quality control test, were normalized using the RMA method. List of >2 fold differentially expressed genes between two classes in p<0.001 significance level were identified (2983 genes in total) using the class comparison tool of the program.

Gene set enrichment analyzes (GSEA) were performed using the GSEA desktop program version 2.0, downloaded from http://www.broadinstitute.org/gsea/downloads.jsp website. Six separate GSEA analyzes were performed using C1 to C6 curated gene set lists downloaded from molecular signature database (MsigDB) and gene expression data of the >2 fold differentially expressed genes of the microarray dataset. Enrichment results of each analysis were further studied.

Table 2.3: *List of curated gene sets and their content.*

Gene Set Name	Collection
C1: positional gene sets	Gene sets corresponding to each human chromosome and each cytogenic band that has at least one gene.
C2: curated gene sets	Gene sets collected from various sources including online pathway databases, publications.
C3: motif gene sets	Gene sets that contain that share a cis-regulatory motif conserved across the human, mouse, rat and dog genomes.
C4: computational gene sets	Gene sets defined by mining large collections of cancer-oriented microarray data.
C5: GO gene sets	Gene sets are named by GO term and contain genes annotated by that term.
C6: oncogenic signatures	Gene sets represent signatures of cellular pathways, often dis-regulated in cancer.

2.3.11 In vivo Tumorigenicity Assay

HepG2 and HepG2-2215 cells (10 million, each) were suspended in 100μL 1X PBS and injected subcutaneously on the back of nude mice; left and right, respectively. And animals were examined for palpable tumors on a weekly basis. After palpable tumors were observed, tumor measurements were done daily. When tumors reached 1 mm^3 volume, the animals were sacrificed and the tumors were taken and were split in to four pieces for further analysis.

2.3.12 Single Cell Isolation from Xenograft Tumors

Firstly, the dissociation buffer was prepared freshly. Then, the subcutaneous tumors were harvested with help of scissors and forceps. Then, the tumor tissues were weighted and appropriate amount of tumor tissues were placed in dissociation buffer. For 1g of tumor tissue, 10mL of dissociation buffer was used. In a sterile biosafety cabinet, tumor tissues were transferred into petri dishes and minced with razor blades. Then tumor cell suspension was titurated through a 5-mL serological pipette 10 times. Then tumor cell suspension transferred into 50mL falcon tube and vortexed for one minute at the highest speed possible. The suspension was incubated at 37℃ for two hours with vortexing 1 minute every 20 minutes. After the incubation, cell suspension was passed through a 40μm strainer and collected in 50mL falcon tube. From this point, cell suspension were seeded or directly fixed for further analysis, such as flow cytometry.

CHAPTER 3

RESULTS

3.1 CD133 as a Cancer Stem Cell Marker in Hepatocellular Carcinoma

CD133 (AC133) is a gene encoding a pentaspan transmembrane glycoprotein. This protein localizes to membrane protrusions and it is generally expressed in adult stem cells. It is thought to function in maintaining stemness. Recently, CD133 expression is associated with several cancer types, including brain tumor, epedymoma, prostate cancer and hepatocellular carcinoma [34]. Previous studies showed that CD133 positivity is associated with proliferation, tumorigenicity, chemo- and radio-resistance [38]. This might be achieved via preferential activation of certain survival pathways. Thus, CD133 is a putative marker which is broadly used in identification of liver CSCs. In our study, it is the primary marker to label the CSC populations.

3.1.1 Screening of Hepatocellular Carcinoma Cell Lines for CD133 Positivity

After CD133 was decided to use as a marker to identify cancer stem cells in hepatocellular carcinoma (HCC), 17 HCC-derived cell lines were screened with immunoperoxidase method. These 17 HCC-derived cell lines were Hep3B and Hep3B-TR, Huh7, PLC/PRF/5, HepG2 and HepG2-2215, Hep40, FLC4, Sk-Hep-1, Focus, Mahlavu, Snu182, Snu387, Snu398, Snu423, Snu449 and Snu475. While HepG2, Huh7, Hep3B and Hep40 were identified as well-differentiated cell lines, other cell lines were either poorly-differentiated or moderately-differentiated cell line [67]. From these 17 cell lines, 6 of them were found to be CD133 positive with different frequencies changing from 10 to 98% (Fig 3.1).These 6 cell lines were

35

Hep3B with 80-90% positivity, Hep3B-TR with more than 90% positivity, Huh7 with 50-70%, PLC with 40-60% and HepG2 with 10-15% positivity and HepG2-2215 with 70-90% positivity. These frequencies were calculated via qualitative observation from immunoperoxidase staining.
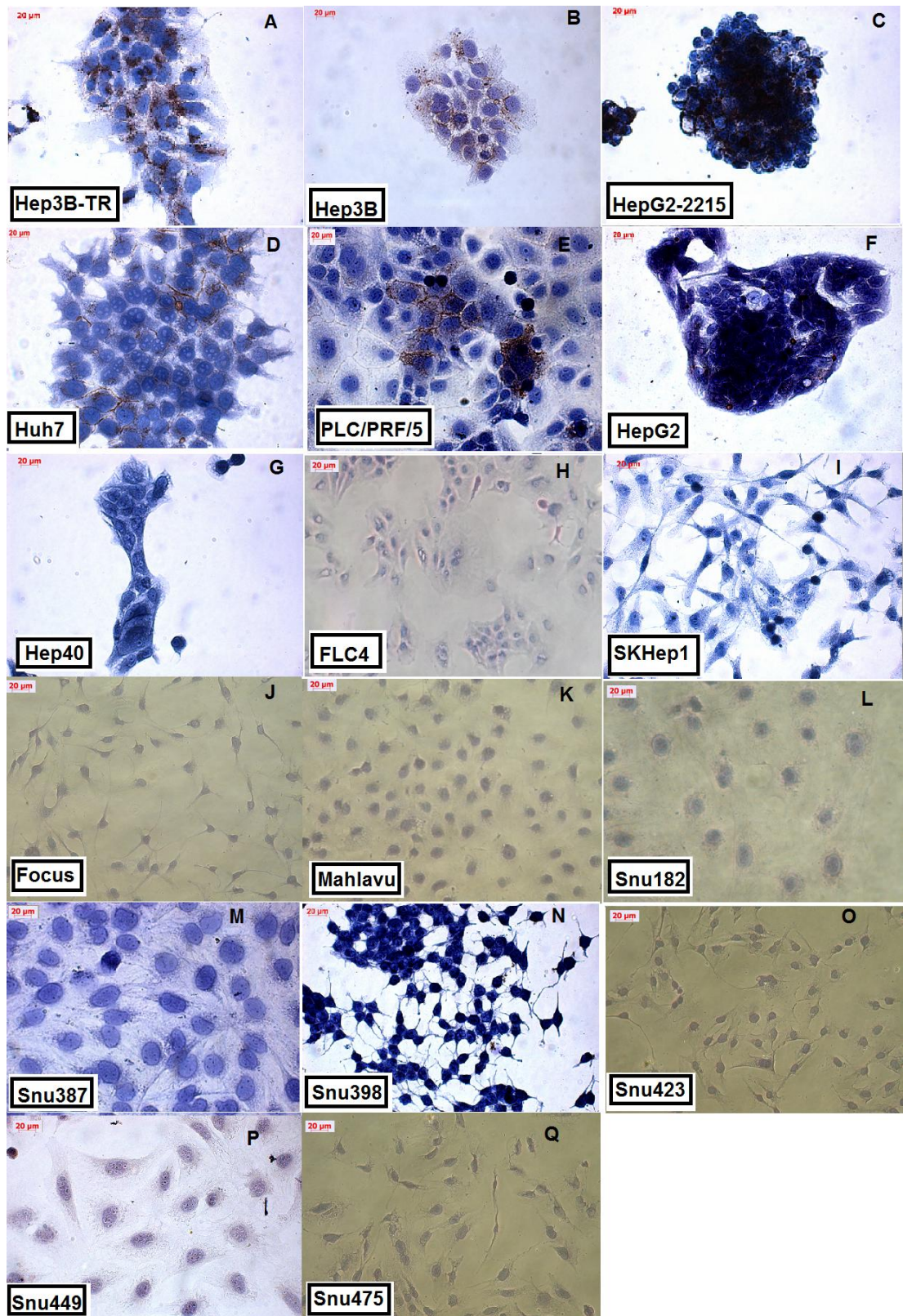
Figure 3.1*: Immunoperoxidase staining of 17 HCC-derived cell lines with CD133 antibody; photomicrographs were taken under bright field microscope, 40X. Cell lines were ranked based on CD133 staining intensities.*

3.1.2 Confirmation of Screening Results by Flow Cytometry Analysis

After the first screening of a set of HCC cell lines, CD133 positivity of these cell lines were also checked by flow cytometry analysis in order to have quantitative results as well as to diminish any error which could be caused in immunoperoxidase experiment that is solely depended on qualitative observation. Thus, all 17 cell lines were analyzed with flow cytometry using CD133-APC conjugated antibody to detect CD133 levels (Fig. 3.2).
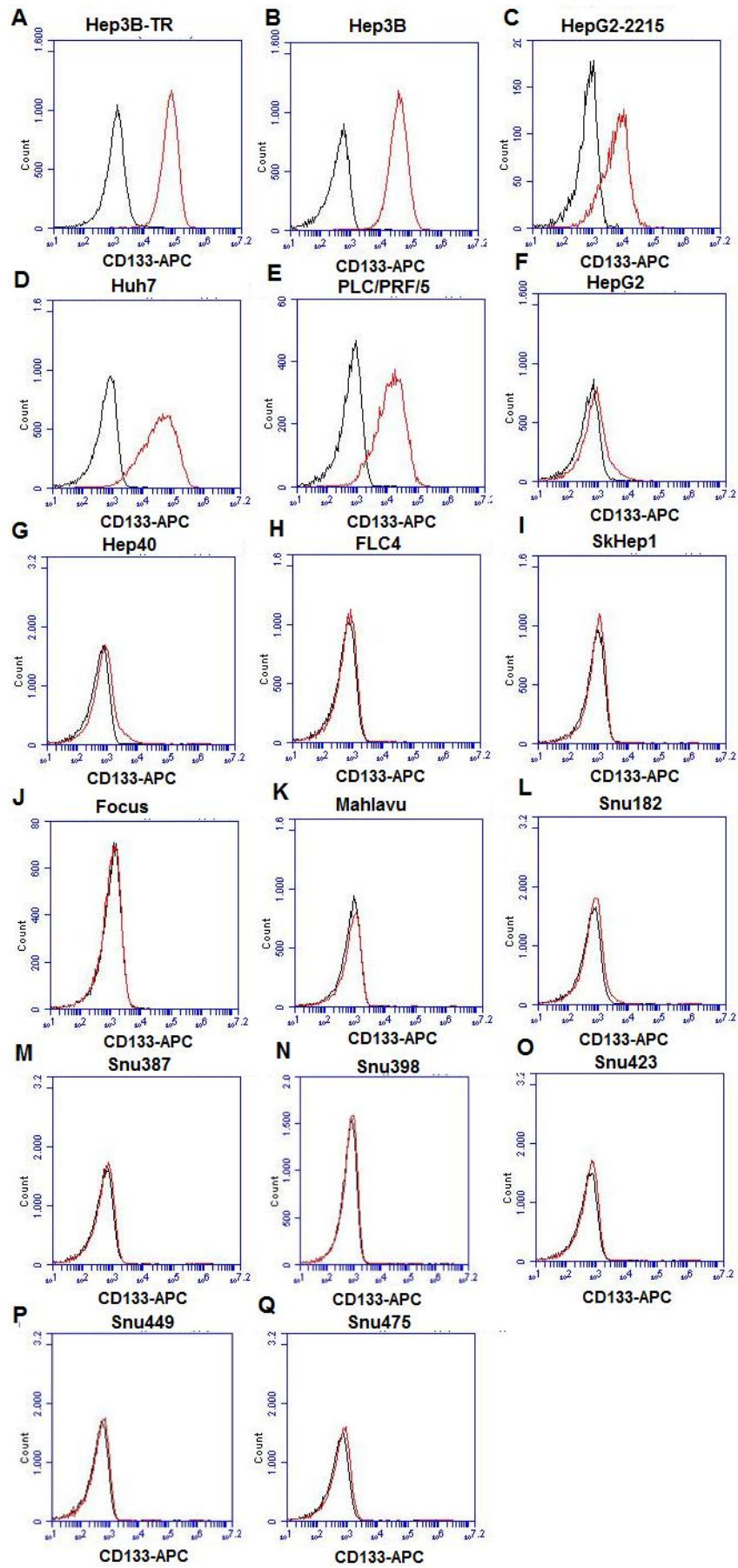
Figure 3.2: Flow Cytometry analysis of 17 HCC cell lines with CD133-APC detection. Cell lines were ranked based on CD133 staining intensities.

These results were consistent with the immunoperoxidase staining data and they also gave us the more accurate percentages of each cell line's CD133 positivity. After these staining methods, cell lines with CD133 positivity were determined according to immunoperoxidase and flow cytometry results (Table 3.1).

Table 3.1: CD133 frequencies of 6 HCC-derived cell lines.

HCC-derived cell line	CD133$^+$ (%) by Immunoperoxidase	CD133$^+$ (%) by Flow cytometry
Hep3B-TR	90-99%	90-99%
Hep3B	80-90%	85-90%
HepG2-2215	70-90%	75-90%
Huh7	50-70%	50-70%
PLC	40-60%	50-60%
HepG2	10%	10-15%

All over, these results suggest that 6 out of 17 HCC-derived cell lines have CD133 positive populations which could be cancer stem cells. Thus, characterization of these CD133+ subpopulations with further investigation was aimed.

3.2 Effects of Different Signaling Pathways on CD133 Positive Population

After the identification of cell lines that possesses CD133 positivity, effects of different signaling pathways were examined. These pathways were chosen because

of their roles in embryonic development, liver development, hepatocellular carcinogenesis and stem cells [42]. Thus, firstly, Wnt signaling was examined. Wnt signaling is a conserved signaling pathway which is linked to hepatocarcinogenesis (Appendix A.1). The second signaling pathway to be examined was TGF-β pathway (Appendix A.2). However, both of these pathways showed a decrease in CD133 levels.

3.3 Studies on HepG2 Parental Cell Line and Its Clone HepG2-2215

As seen in Appendix A.1 & A.2, investigation of two signaling pathways revealed an inverse relationship which was unexpected because of the literature. These findings along with two isogenic cell lines with differential CD133 expression prompted us to focus on these two cell lines; parental HepG2 and its clone, HepG2-2215 (Appendix A.1 & A.2). HepG2 is an adherent cell line which grows in small aggregates, it is epithelial-like and from a 15-year-old male. Meanwhile HepG2-2215 is a clone of HepG2 which is transfected with four 5'-3' tandem copies of the hepatitis B virus (HBV) genome positioned such that two dimers of the genomic DNA are 3'-3' with respect to one another. Thus, HepG2-2215, expresses Hepatitis B e antigen and Hepatitis B surface antigen. Immunoperoxidase and flow cytometry analysis showed that while HepG2 have 10-15% CD133 positivity, in HepG2-2215 cell line, CD133 ratio is between 70-90% (Figs. 3.1 & 3.2).

It was very surprising that while parental cell line has low CD133+ cell population, its clone has around 80% positivity. This increase in CD133 levels might be caused by HBV infection. However, to be sure that the CD133 positive cell frequency of HepG2-2215 is high as 80%, another marker, namely EpCAM, to detect stemness more strictly, was used. EpCAM is normally expressed in epithelial cells and it is a carcinoma-associated antigen which is widely used in CSC studies. HepG2 and HepG2-2215 cell lines were stained with both CD133 and EpCAM markers to detect CSCs in a more defined way (Fig. 3.3).
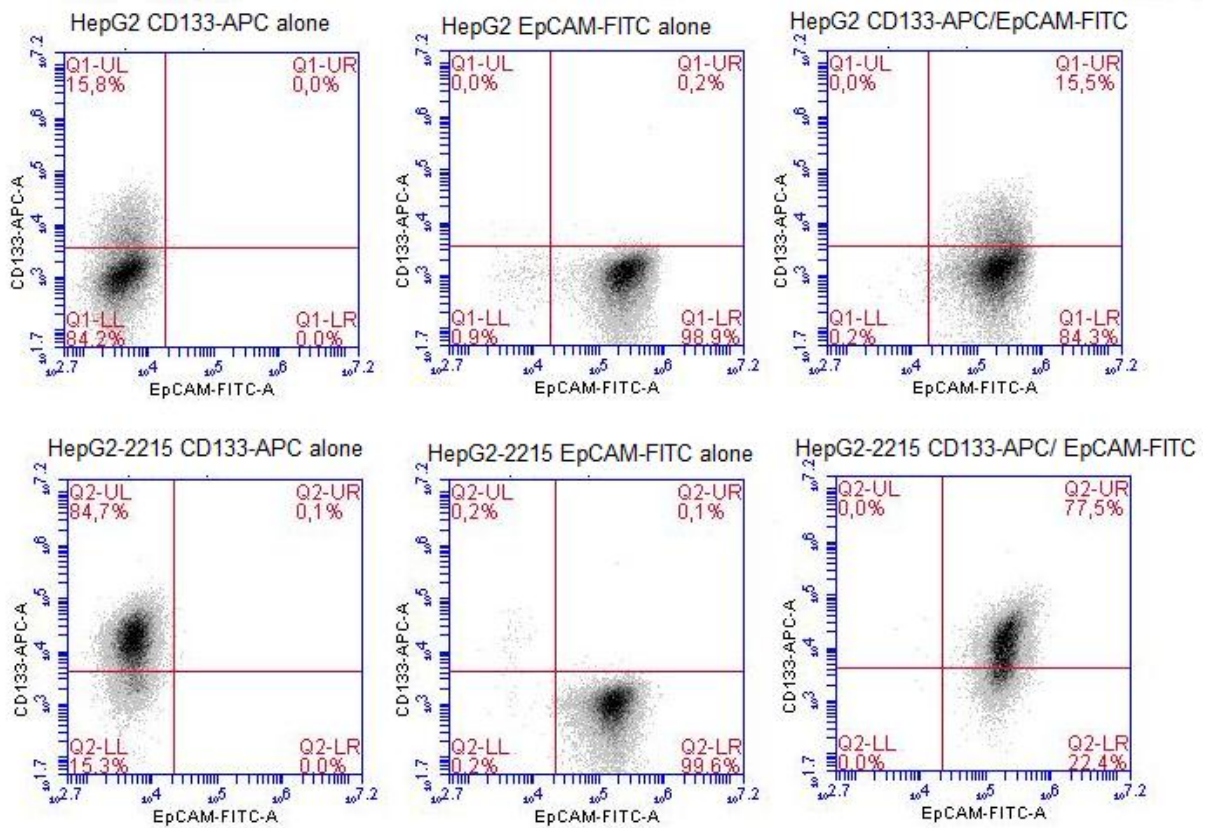
Figure 3.3: *Detection of CD133⁺ and/or EpCAM⁺ subpopulations in parental HepG2 and its derivative HepG2-2212 cell lines by flow cytometry analysis.*

This data showed that while these two cell lines showed no difference in EpCAM positivity, HepG2-2215 cell line has significantly more double positive cells which supports that this cell line has more cancer stem cells than HepG2 cell line.

3.3.1 Effects of Serum Starvation Model on HepG2 and HepG2-2215 Cell Lines

After this remarkable difference in CD133 positivity between HepG2 and its clone HepG2-2215 was found, further studies were performed. Up to this point, all experiments were done with serum starvation model. The aim of using serum starvation model was to create harsh conditions where normal cancer cells will start to die while cancer stem cells will endure these conditions and would remain healthy.

This way we could assess if serum starvation was affecting CD133 positivity. The cells were seeded on day zero with complete medium and on day 1, they were harvested and fixed for FACS analysis. In a parallel plate, cells were first kept under complete medium for a day and then, transferred to serum starvation media for additional three days (day 4). On day 4, they were fixed and analyzed by flow cytometry analysis (Figs 3.4 & 3.5).

This analysis showed that while serum starvation model did not affect the HepG2-2215 cell line, this model decreased the CD133 positivity ratio of HepG2 cell line, unexpectedly (Fig. 3.4).
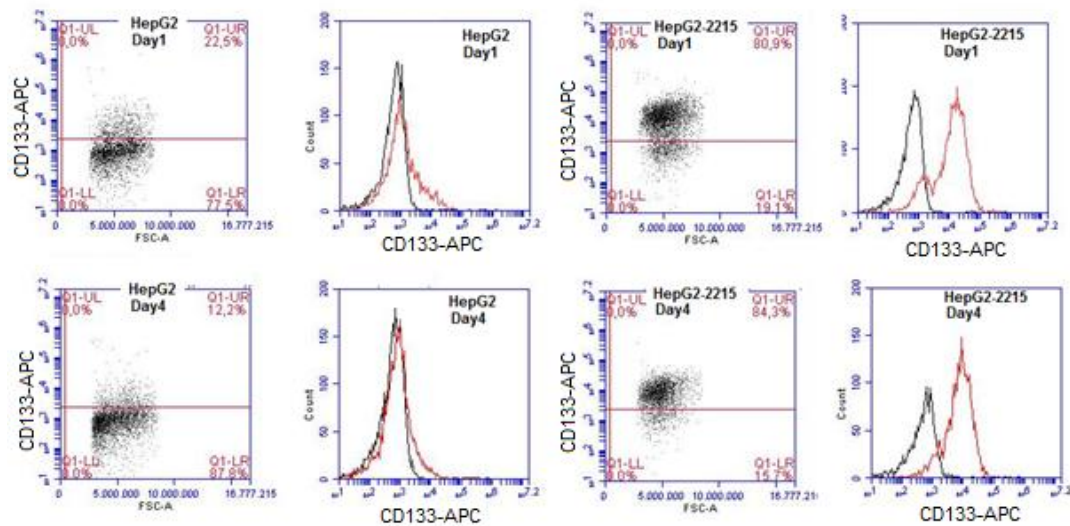
Figure 3.4: *Effects of serum starvation model on CD133 levels of HepG2 and HepG2-2215 by flow cytometry analysis.*

To have more accurate results and differentiate real stemness, double staining with CD133 and EpCAM were performed to observe effects of serum starvation method on CSCs (Fig. 3.5). These data showed that in single staining, CD133$^+$ cell frequency dropped significantly in HepG2 only (Fig. 3.4). However, double staining revealed that HepG2-2215 was also affected from serum starvation with a reduction from 90% cells to 80% double positivity (Fig. 3.5). On the other hand, decrease in HepG2 cell

line was much more significant. Double positive cell number of HepG2 diminished from 10% to 2.5 % (ca. 75% decrease).
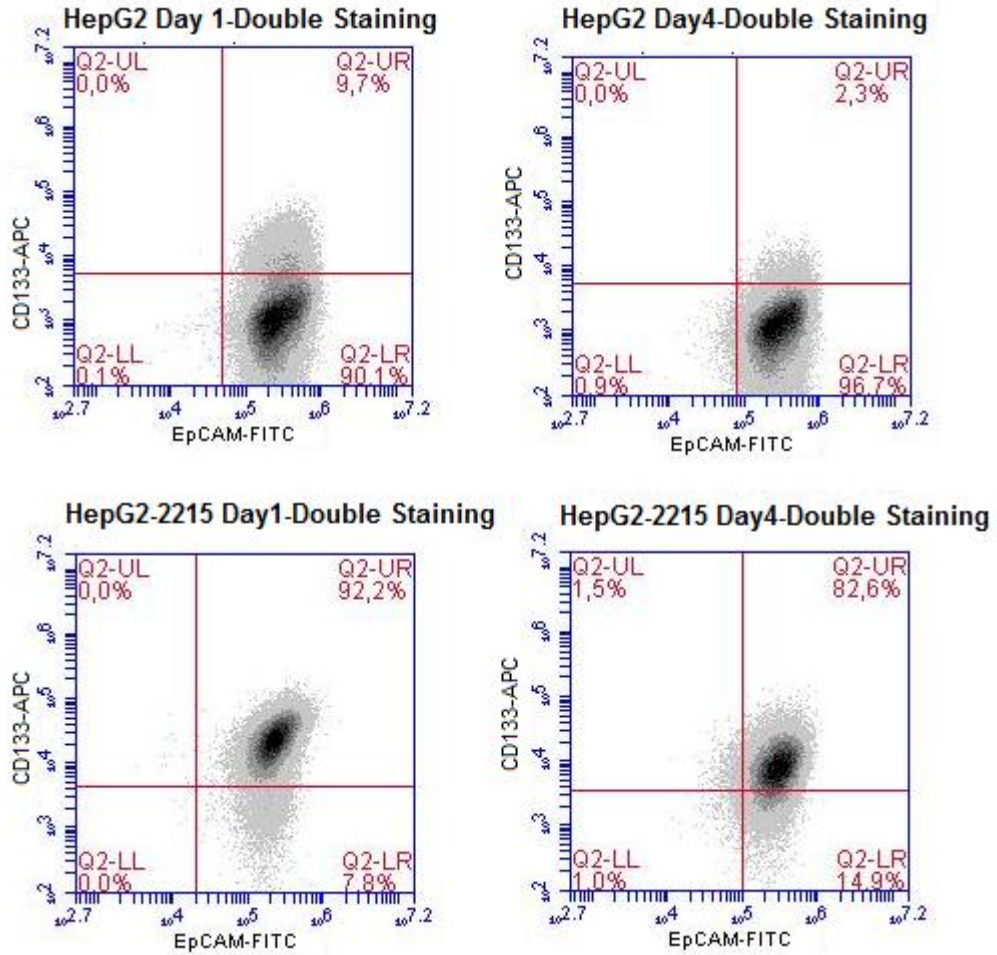
Figure 3.5: *Effects of serum starvation procedure on CD133/EpCAM levels of HepG2 and HepG2-2215 by flow cytometry analysis.*

3.3.2 Efforts to delineate differential expression of CD133 between HepG2 and HepG2-2215

After it is found that HCC-derived cell line HepG2 has 10-20% CD133 positivity while its clone HepG2-2215 has 70-90% positivity, identifying the reason of this difference is the main question. This difference can depend on the fact that the origin of the HepG2-2215 clone may be a positive HepG2 cell or this positivity might be gained with the HBV transfection and the following consequences. So, the biggest question was to find out the reason why HepG2-2215 has higher CD133 positivity than HepG2. To address this question, firstly, soluble factors were examined through a simple setup. It is hypothesized that any soluble factor that leads to an increase in CD133 positivity in HepG2-2215 cell line should be available in its medium and HepG2-2215 medium-treated HepG2 should show advanced CD133 positivity. To test this, HepG2 cell line was grown in normal complete medium or it was treated with either HepG2 medium which was collected from HepG2 cell line after 3 days or HepG2-2215 medium which was collected after 3 days (Fig. 3.6). Media were added to HepG2 for treatment in serial dilutions (1/1, 1/2 and 1/4) and treatment lasted for 10 days. This was also conducted for HepG2-2215 cell line to observe effects of HepG2 or HepG2-2215 media (Figs. 3.6 & 3.7).
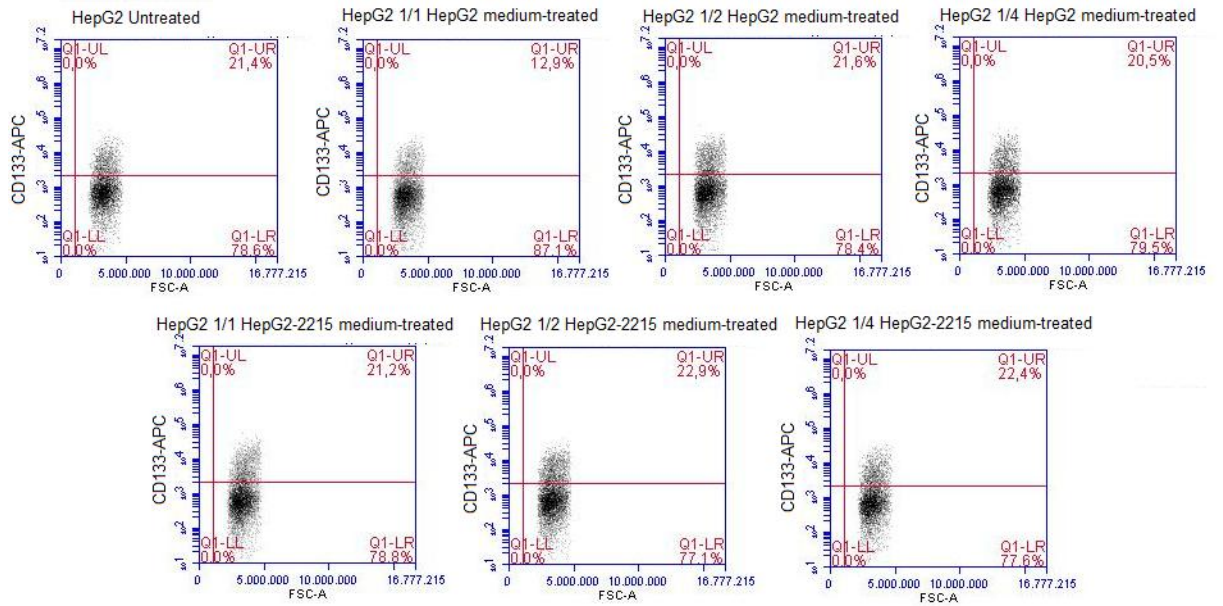
Figure 3.6: *Possible effects of soluble factors from HepG2 and HepG2-2215 media on CD133 levels in HepG2 by flow cytometry analysis.*
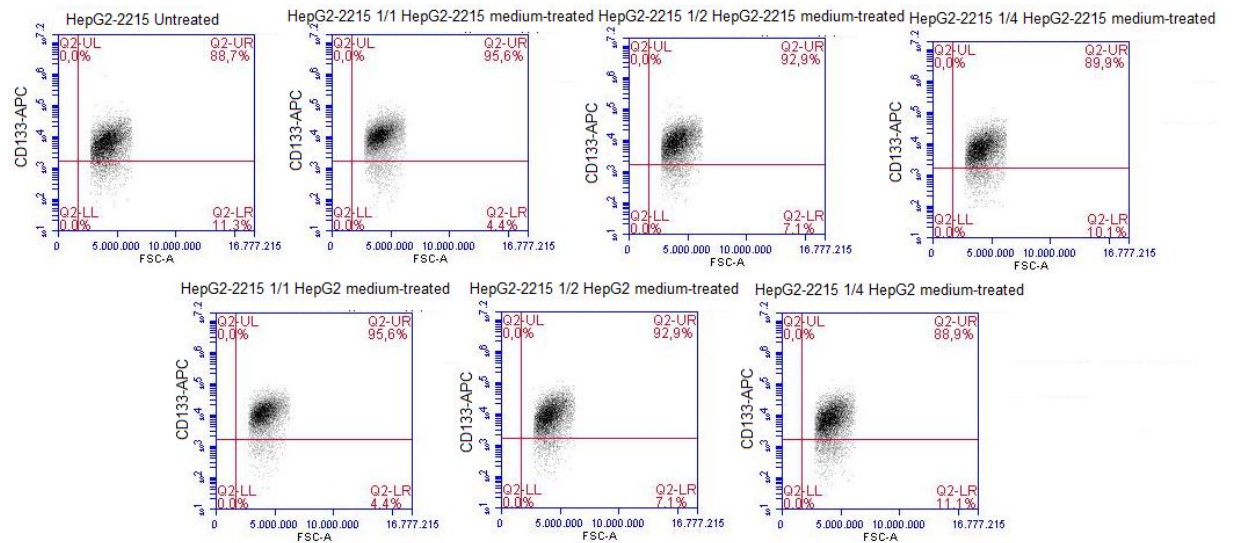
Figure 3.7: *Possible effects of soluble factors from HepG2 and HepG2-2215 media on CD133 levels in HepG2-2215 by flow cytometry analysis.*

These findings suggested that CD133 levels of HepG2 and HepG2-2215 were not affected by any soluble factor which might be present in media. Thus, it can be

concluded that the difference of CD133 positivity of these two cell lines does not depend on any soluble factor.

3.3.3 Efforts to Understand the Relatedness of Oval Cells with CSCs

Recent data showed that hepatocytes became oval cells in response to Notch signaling activation or injury that provokes a biliary response and then these oval cells differentiate into biliary epithelial cells [68]. The mammalian liver is an exceptional regenerative organ that following a toxin-mediated injury, exhibits an accumulation of atypical ductal cells (ADCs) which are also referred as "oval cells" [68]. Oval cells are intra-hepatic stem cells with bi-potentiality and they can give rise to two types of epithelial cells in liver; hepatocytes and bile ductular cells [69, 70]. In that study, HNF4α was used as a hepatocyte marker while Sox9 was the biliary epithelial cell marker. Thus, expression of both of these markers was the sign of oval cells with a bi-potential stemness. Oval cells may give rise to CSCs, and possessing more oval cells indicates stemness-rich nature. To observe if HepG2 and HepG2-2215 also express these two markers; HNF4α and Sox9 to validate their stemness, a Western blot analysis was performed in HepG2 and HepG2-2215 cell lines that were collected from day1 or day4 that was serum-free medium treated (Fig. 3.8).
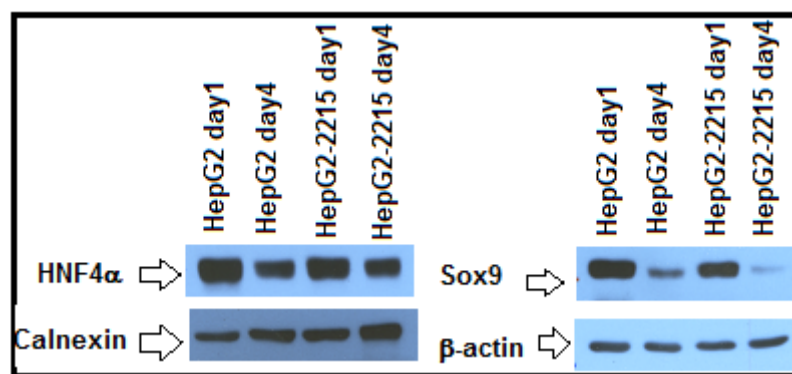
Figure 3.8: *Expression levels of HNF4α and Sox9 in HepG2 and HepG2-2215 cell lines by Western blot.*

From the Western blot analysis, HepG2 and HepG2-2215 cell lines showed that they have different amounts of Sox9 expression where HepG2 showed higher expression levels. The expression levels of Sox9 in these two cell lines decreased when cells were treated with serum starvation model. For HNF4α expression, it seemed like that HepG2 had higher levels of HNF4α expression than HepG2-2215, and their expression levels also decreased with serum starvation model. Even though, as total expression levels, HepG2 expresses both Sox9 and HNF4α in higher amounts, the important point was to identify cell number that express both markers in these cell lines. To investigate double positive cells, which indicate presence of oval cells, an immuno-fluorescence experiment was conducted on HepG2 and HepG2-2215 cell lines (Fig. 3.9).
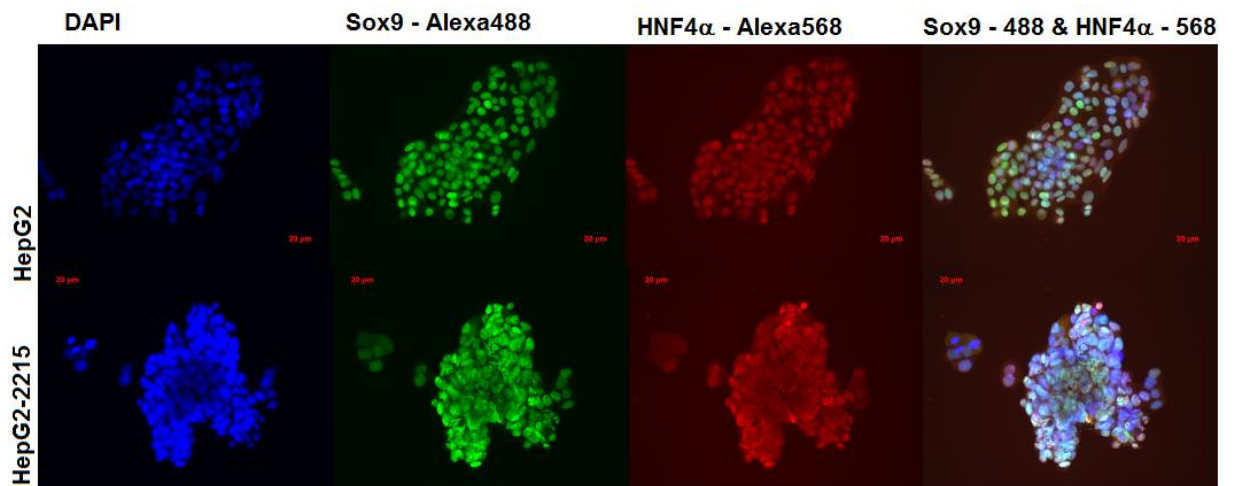
Figure 3.9: *Expression levels of HNF4α and Sox9 in HepG2 and HepG2-2215 cell lines by Immunofluorescence. Fluorescent microscopy, 40X.*

Immunofluorescence staining data showed that HepG2-2215 cell line had more double positive cells for Sox9 and HNF4α than HepG2 cell line. This also implied that HepG2-2215 cell line has more cells with bi-potentiality that demonstrated its stemness-rich nature.

3.4 Effect of CD133$^+$ Levels on Tumor Formation Ability

Since HepG2-2215 cell line showed higher levels of CD133 and EpCAM positive subpopulation and more double positive cells for Sox9 and HNF4α, CSC subpopulation in HepG2-2215 was bigger than HepG2. Thus, HepG2-2215 should be able to form a bigger tumor than HepG2 cell line. Also, it was expected that when injected to a mice, HepG2-2215 cell line would show a more rapid tumor growth than HepG2 cells. To investigate this, a tumorigenicity assay was conducted on 5 male, atymic, nude mice where HepG2 cells were injected to the left side of the mice while HepG2-2215 cells were injected to right side. After injections, first tumor growth was observed at day 15 post injection and then, tumor growth kinetics were observed (Figs. 3.10).
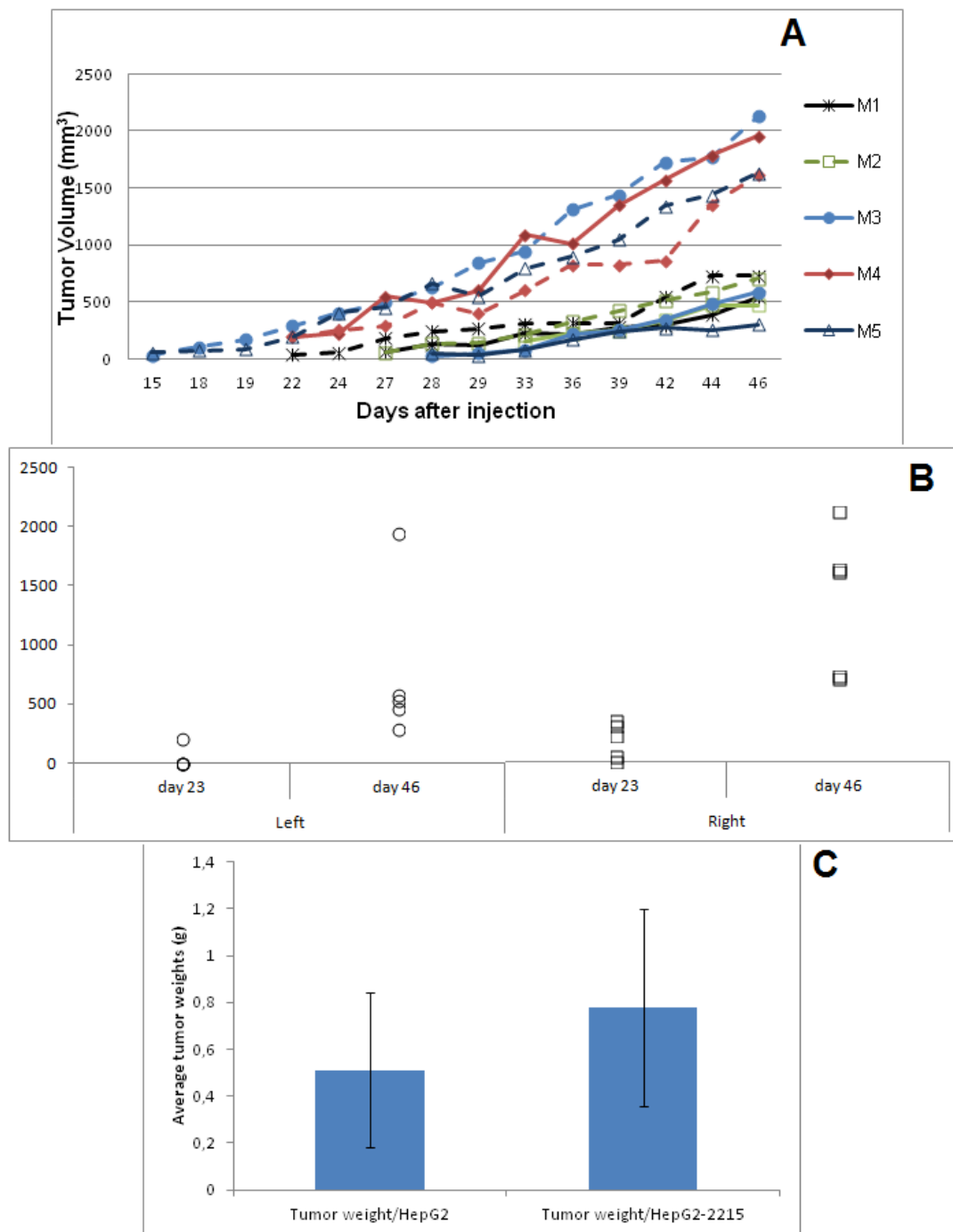
Figure 3.10: *A) Tumor growth kinetics of HepG2 and HepG2-2215 cell lines. (Bold lines, left side/HepG2; dashed lines, right side/HepG2-2215). B) Comparison of tumor volumes of HepG2 or HepG2-2215 derived tumors on day 23 and day 46. C) Average tumor weights of tumors derived from HepG2 or HepG2-2215.*

Palpable tumors were observed at day 15 after injection and from that point; tumors were measured three times a week (Fig. 3.10). When the tumor volumes have reached more than 1000 mm^3, animals were sacrificed and tumors were collected. Their weights were also measured to see if the volume and the weight were consistent with each other or not (Fig. 3.10.C).Tumor photos were shown in Figure 3.15. In 4 out of 5 mice, right side tumor was bigger than left side.

Left - HepG2 **Right - HepG2-2215**

Mice 1

Mice 2

Mice 3

Mice 4

Mice 5
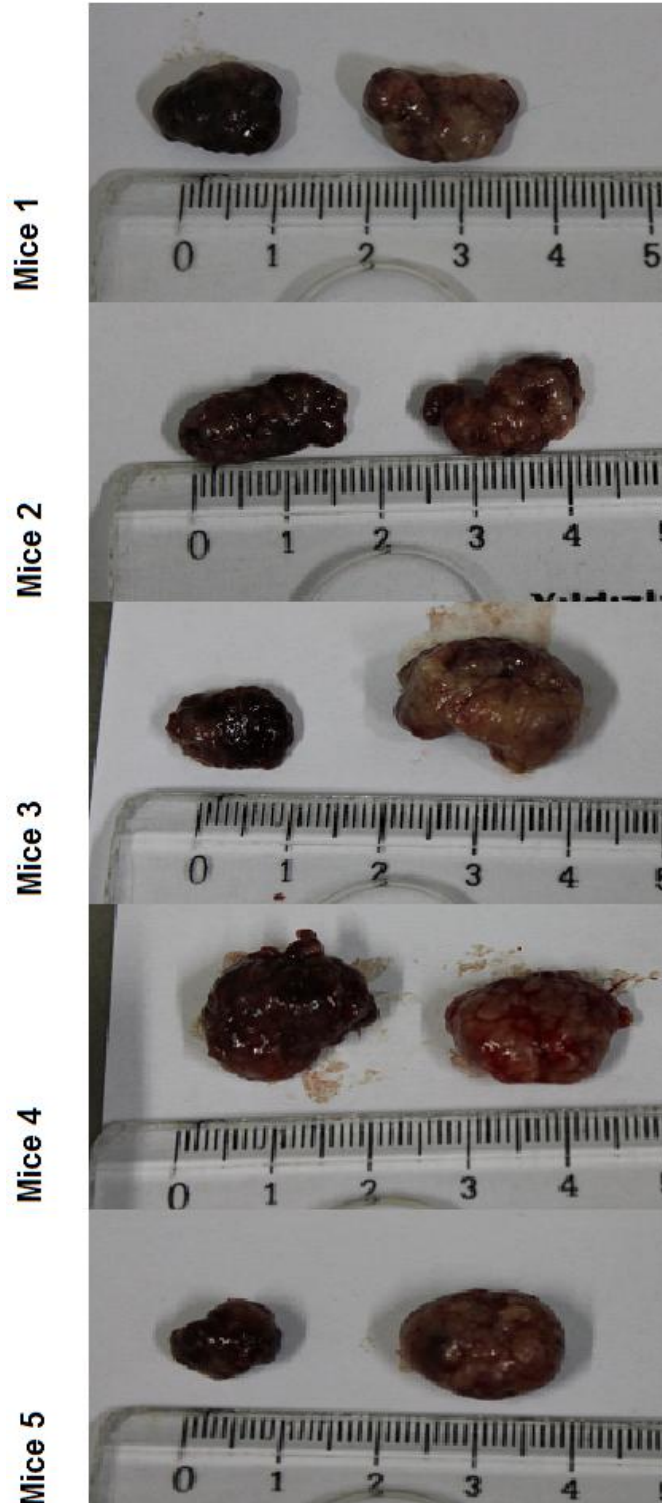
Figure 3.11: *The representative photos of tumors that were collected from xenograft nude mice.*

Tumorigenicity assay showed that HepG2-2215 cell line has higher tumor formation ability than HepG2 cell line as expected. HepG2-2215-derived tumors were observed earlier than HepG2 (Fig. 3.10.A). Moreover, their volumes were also higher than HepG2-derived tumors (Fig. 3.10.B). Another observation from this experiment was that the appearances of tumors were significantly different from each other. While tumors derived from HepG2 cells showed darker color implying more blood vessels in the tumor environment, HepG2-2215-derived tumors showed lighter color and they appeared to have more lipids in the tumor environment (Fig. 3.11).

3.4.1 Flow Cytometry Analysis of Xenograft Tumor Tissues

In tumorigenicity assay, after tumors were taken, they were split into four equal pieces for further studies. Firstly, cells were dissociated to obtain single cell suspension and then, these cells were stained with CD133-APC to observe their CD133 positivity levels (Fig. 3.12).
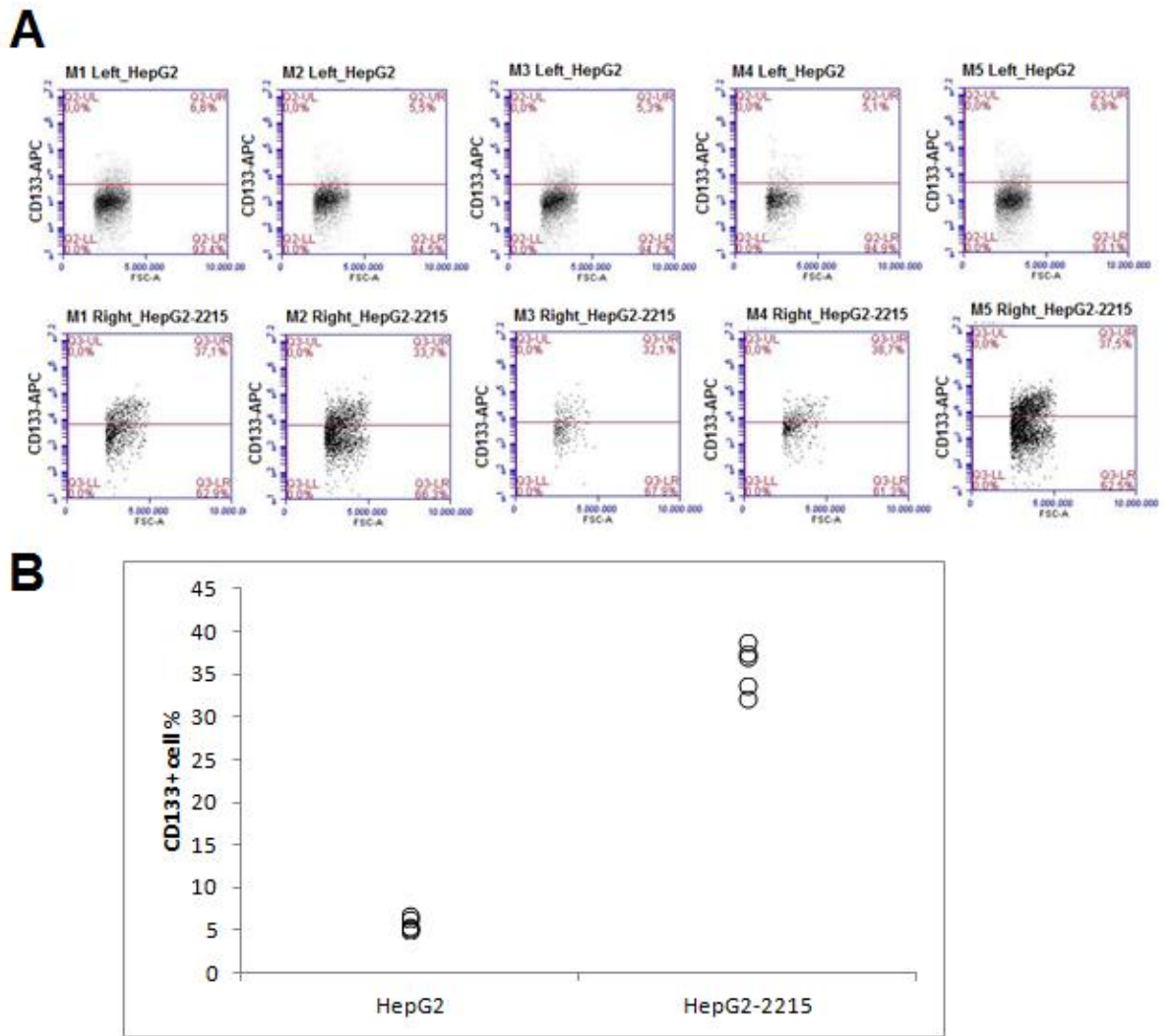
Figure 3.12: *Differential CD133$^+$ levels of HepG2- and HepG2-2215-derived tumors.*

This analysis showed that while HepG2-derived tumor cells had 5-7% CD133 positivity, HepG2-2215-derived tumor cells had 30-40% CD133 positivity (Fig. 3.12). This supported the view of the HepG2-2215 cell line has more cancer stem cells which resulted in more rapid tumor growth in xenograft study.

After it has been shown that HepG2-2215 cell line had more CD133 positivity even after xenograft study, these tumor masses were further investigated with CD133/EpCAM staining with flow cytometry to detect CSCs more accurately with two markers (Fig. 3.13). Also, to characterize tumor microenvironment, M1/M2

macrophages were also checked by flow cytometry using CD86 for M1 macrophage marker and CD206 for M2 macrophage marker (Appendix Fig. A3.5).
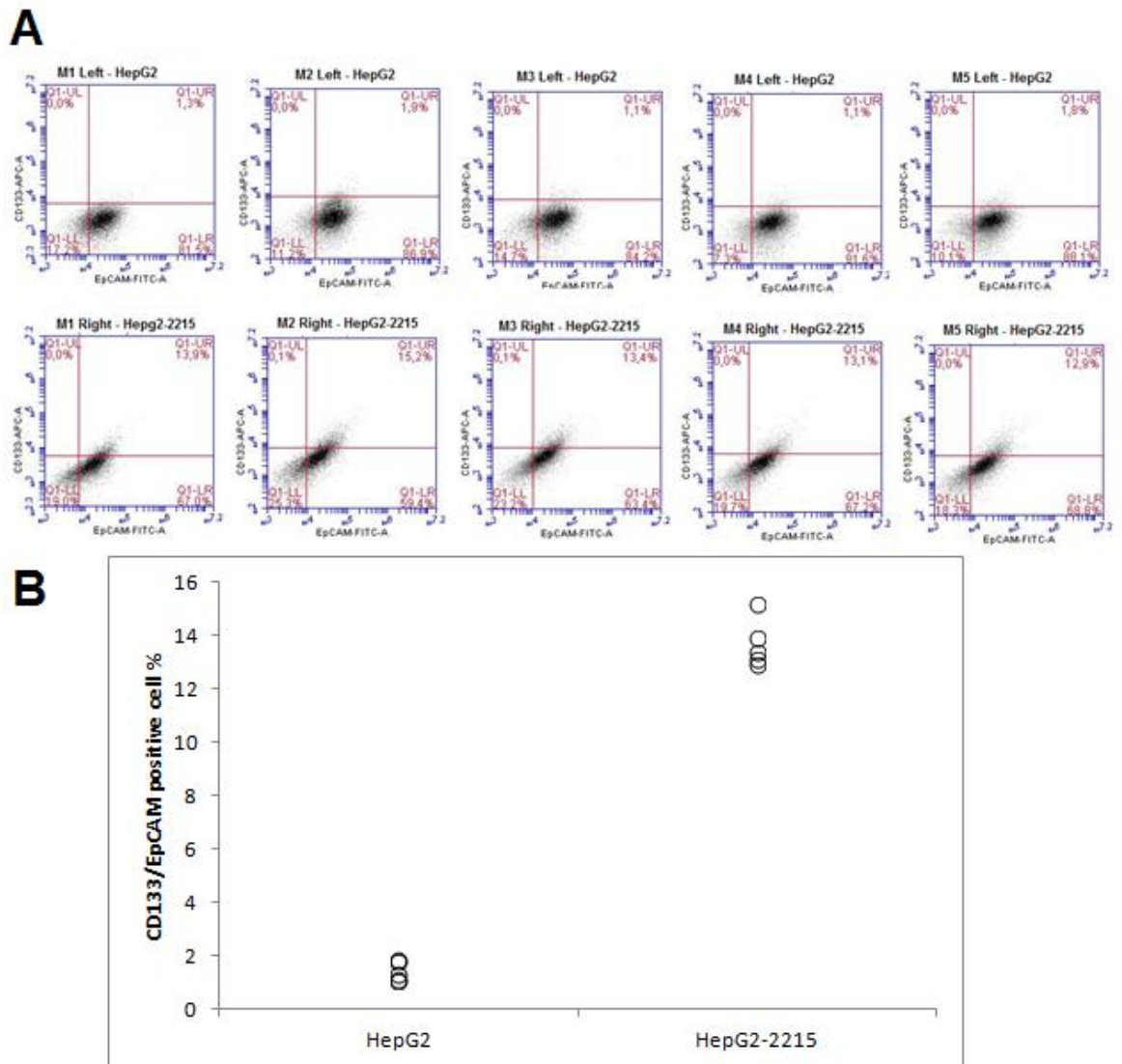
Figure 3.13: *Differential CD133/EpCAM levels of HepG2- and HepG2-2215-derived tumors.*

These data suggested that even after xenograft studies, HepG2-2215 continued to have higher double positive cell ratio for CD133 and EpCAM than HepG2 cell line. This implied that HepG2-2215-derived tumors have more cancer stem cells which cause more rapid tumor initiation and these cells also might help the maintenance of the tumor.

3.5 Microarray Study between HepG2 and HepG2-2215 Cell Lines

To have a better understanding of what caused the higher levels of CSCs in HepG2-2215 cell line, a microarray study between HepG2 and HepG2-2215 cell lines was conducted from triplicate samples (Fig. 3.14). Then, genes with at least 1.5 fold changes in expression took into consideration for further studies.
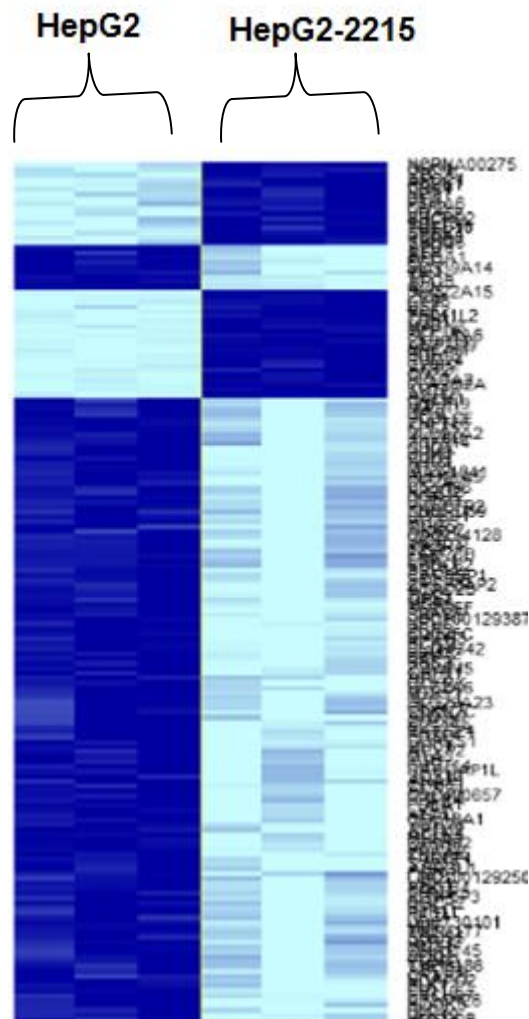
Figure 3.14: *Representative heatmap of microarray analysis between HepG2 and HepG2-2215 cell lines.*

Microarray analysis revealed that 4486 genes were expressed differentially, while 1926 of them were up-regulated in HepG2-2215 cell line.

2983 differentially expressed genes with more than 2 fold change and p< 0.001 significance value between HepG2 and HepG2-2215 cell lines were analyzed with GSEA (Gene Set Enrichment Analysis) method. C1, C2, C3, C4, C5, and C6 curated gene set lists were separately analyzed (Table 2.3 & 3.3).

Table 3.3: List of gene numbers that were enriched in either HepG2 or HepG2-2215 in curated gene set lists.

Cell line with enrichment	C1 (330)	C2 (4555)	C3 (826)	C4 (837)	C5 (1363)	C6 (189)
HepG2-2215	140	2770	516	463	819	113
HepG2	163	1785	310	374	544	76

In order to simplify the complex GSEA results for easier interpretation enrichment pathway maps were generated based on lists of enriched genes in each gene sets using the Cytoscape pathway generation program with Gökhan Yıldız (personal communication). The pathways were generated for each curated gene set lists. Gene sets in the pathways and genes causing pathway interactions in the gene sets were further investigated using the data of the maps of the each pathway. Gene sets were categorized in four groups for further analyzes; development/differentiation, signaling, stem cell, and virus/HCC/cancer. 73 gene sets in total were determined using this method (Appendix Table A4.1, A4.2, A4.3 & A4.4). With the help of these data, more meaningful results were obtained that led to a focus on FGFR signaling pathway.

3.5.3 FGFR Signaling Pathway

After microarray analysis, it has been shown that FGFR signaling pathway was significantly up-regulated in HepG2 cell line. All four FGF receptors, FGFR1, FGFR2, FGFR3 and FGFR4 were down-regulated in HepG2-2215 cell line (Table 3.4). In addition to the receptors, FGFR signaling ligand FGF2 were also down-regulated in HepG2-2215 cell line.

Table 3.4: *Differentially expressed FGFR signaling pathway.*

Gene Symbol	Probe set ID	Fold change (HepG2-2215/HepG2)	Fold change (HepG2/HepG2-2215)
FGF13	205110_s_at	122,3173	0,0082
FGFR3	204379_s_at	0,611131	1,64
FGFR1	211535_s_at	0,407627	2,45
FGFR4	204579_s_at	0,398808	2,51
FGFR2	203638_s_at	0,208346	4,8
FGF2	204422_s_at	0,085947	11,63

Differential expression of FGFR signaling pathway genes were studied with Western blot technique using P-FGFR antibody, which recognizes phosphorylated FGF pathway receptors including FGFR1, FGFR2, FGFR3 and FGFR4 (Figs. 3.15 & 3.16). Firstly, both HepG2 and HepG2-2215 cell lines were analyzed for their phosphorylated FGFR levels with Western blot technique (Fig. 3.15).
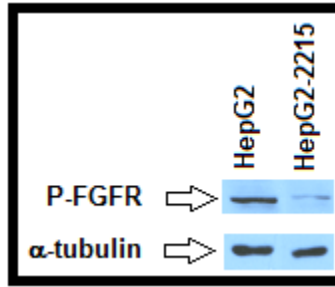
Figure 3.15: *Expression levels of P-FGFR in HepG2 and HepG2-2215 cell lines by Western blot analysis.*

Because serum starvation model was used in most of the analysis, protein of HepG2 and HepG2-2215 cell lines that were collected from day1 (untreated) and day4 (serum starvation treated). And Western blot analysis was repeated for these samples (Fig. 3.16).
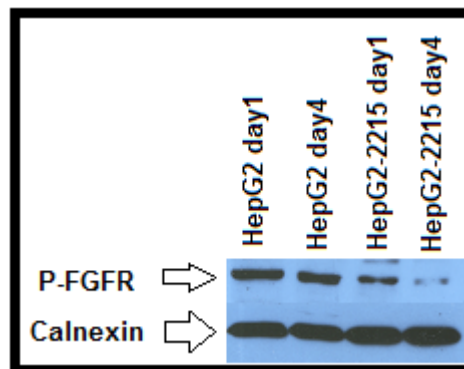
Figure 3.16: *Expression levels of P-FGFR in HepG2 and HepG2-2215 cell lines by Western blot analysis.*

These findings showed that HepG2 cell line indeed has higher levels of P-FGFR than HepG2-2214, and as expected P-FGFR levels decreased in both cell lines upon serum starvation treatment. However, this decrease more significantly in HepG2-2215 cell line which makes a bigger difference in P-FGFR levels in these two cell lines (Fig. 3.16).

3.5.3.1 Inhibition of FGFR Pathway

HepG2 cell line has low levels of CD133+ cells and its FGFR signaling is up-regulated while HepG2-2215 has high levels of CD133+ cells and FGFR signaling is down-regulated. This differential expression of CD133 and FGFR signaling pathway genes might affect each other in a reverse fashion. To investigate the relationship between FGFR signaling pathway and CSCs, HepG2 and HepG2-2215 cell lines were treated with SU5402 which is a potent FGFR inhibitor. Two different concentrations of SU5402 (2μM and 10μM) were used for 48 hours treatment. After the treatment, cells were collected and fixed for flow cytometry analysis (Fig. 3.17 & 3.18). Cells were stained with CD133-APC, EpCAM-FITC and FGFR2 antibody that is conjugated to Alexa488 with Lightning-Link kit (Fig. 3.17 & 3.18).
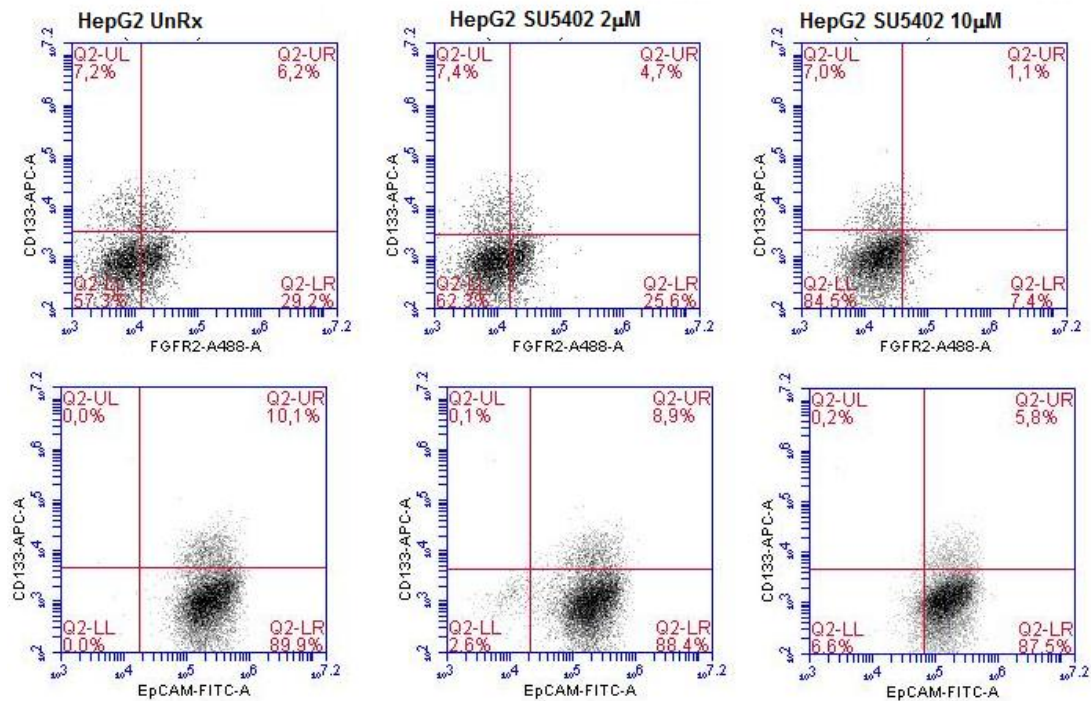
Figure 3.17: *Effects of inhibition of FGFR signaling pathway via SU5402 treatment for 48 hours on CD133/EpCAM levels in HepG2 by flow cytometry.*
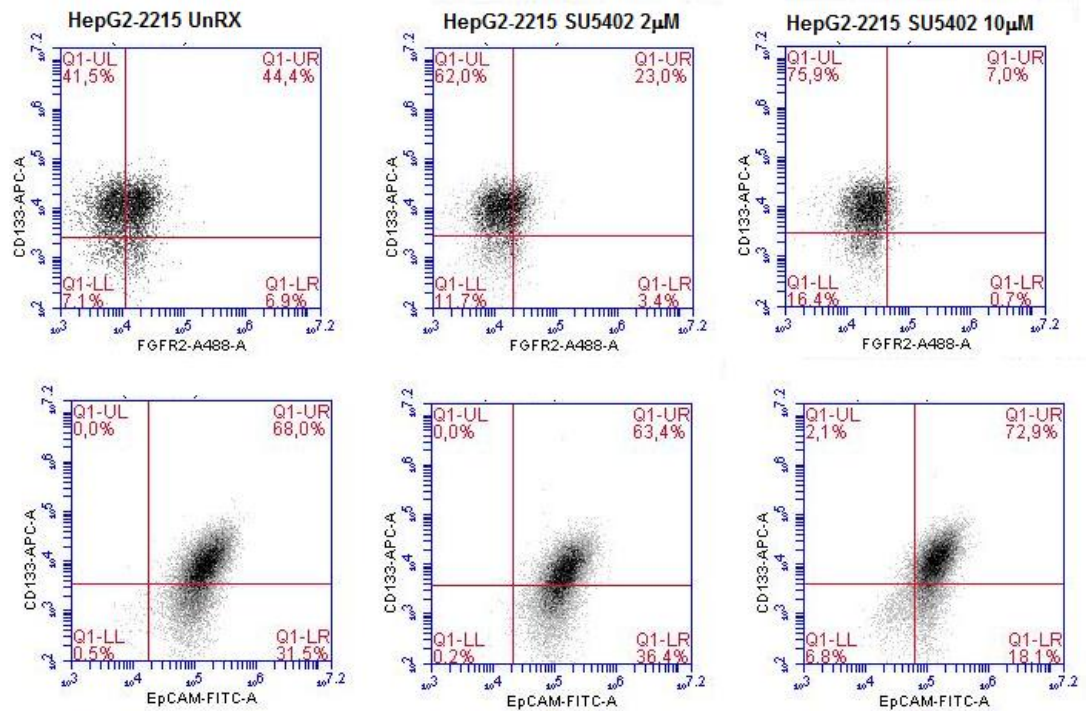
Figure 3.18: *Effects of inhibition of FGFR signaling pathway via SU5402 treatment for 48 hours on CD133/EpCAM levels in HepG2-2215 by flow cytometry.*

These results showed that inhibition of FGFR signaling via SU5402 treatment decreased FGFR levels in both HepG2 and HepG2-2215 in dose-dependent manner. However, this decrease in FGFR levels was affected CD133/EpCAM levels in only HepG2 cell line, while HepG2-2215 showed inconsistency in its CD133/EpCAM levels with increasing SU5402 dose (Fig. 3.17 & 3.18). Unfortunately, in HepG2, CD133/EpCAM levels dropped with decreasing FGFR levels, which is unexpected (Fig. 3.17).

3.5.3.2 siRNA Knockdown of FGFR2

After FGFR inhibition via SU5402, this time, FGFR signaling pathway was inhibited by siRNA knockdown of FGFR2. For this, a pool of siRNAs targeting FGFR2 was used in different concentrations ranging from 12.5nM to 100nM in 2X dilutions. Cells were reverse transfected and after 72 hours treatment, cells were collected for flow cytometry (Fig. 3.19 & 3.20). Again, CD133, EpCAM and FGFR2 levels were checked.
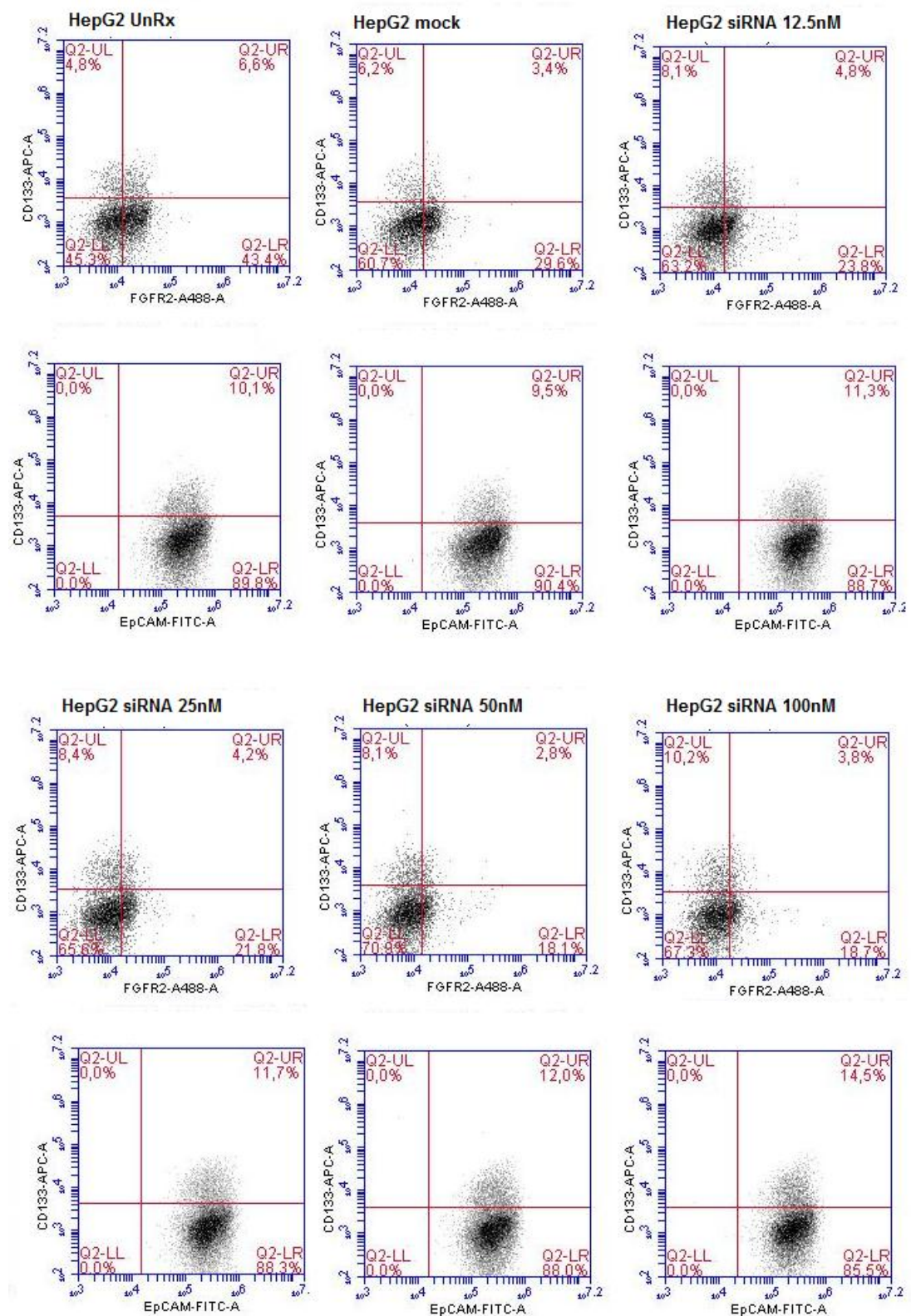
Figure 3.19: *Effects of inhibition of FGFR signaling pathway via siRNA treatment against FGFR2 on for 72 hours CD133/EpCAM levels in HepG2 by flow cytometry.*
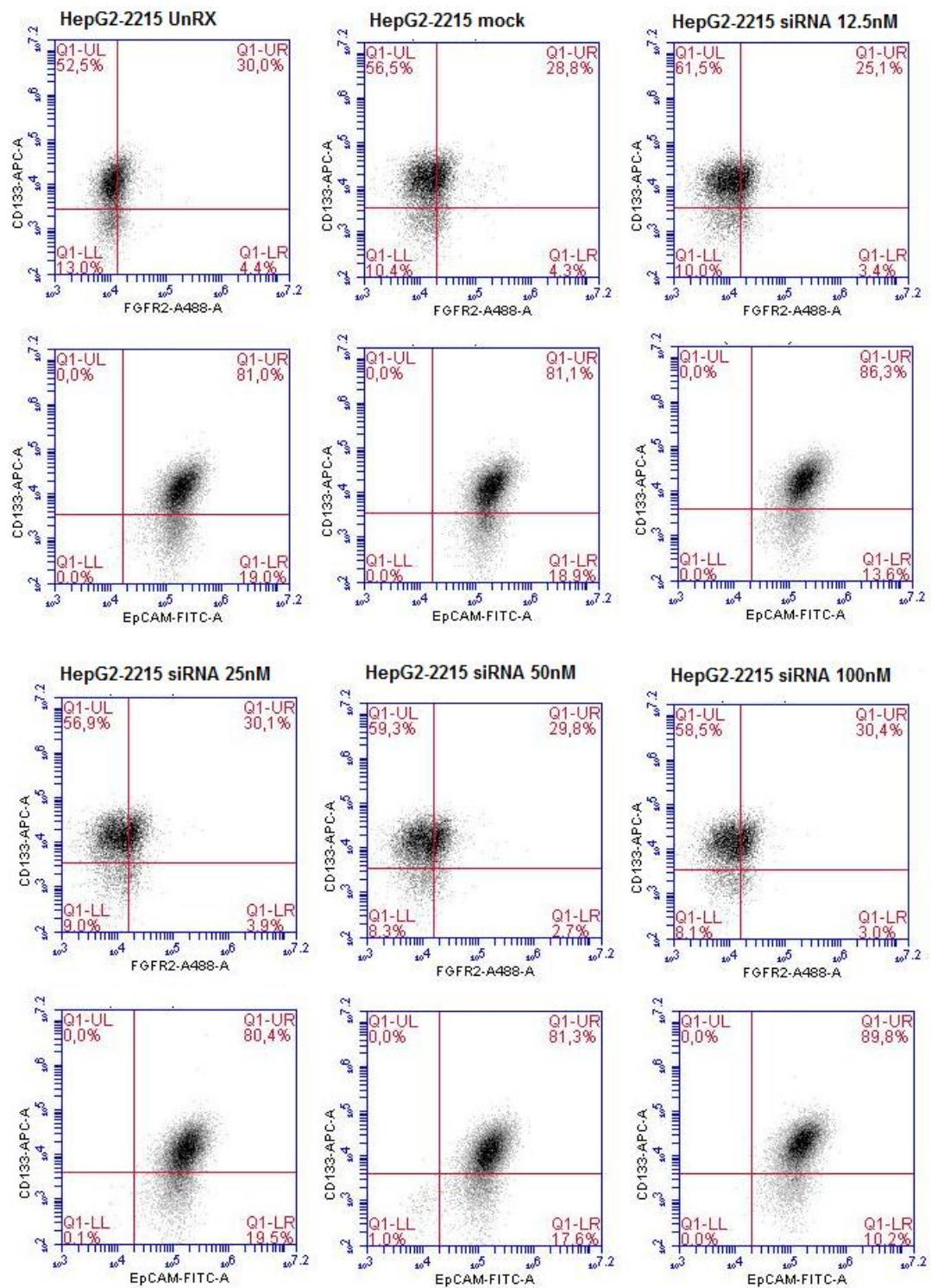
Figure 3.20: *Effects of inhibition of FGFR signaling pathway via siRNA treatment against FGFR2 for 72 hours on CD133/EpCAM levels in HepG2-2215 by flow cytometry.*

These results showed that in HepG2 cell line, there was a decrease in FGFR2 levels with siRNA treatment in a dose-dependent manner. However, this was not observed in HepG2-2215 cell line. In HepG2 cell line, it is observed that with decreasing levels of FGFR2, CD133/EpCAM levels showed a slight increase (Fig. 3.19). CD133/EpCAM levels in HepG2-2215 demonstrated inconsistent up and downs upon siRNA treatment (Fig. 3.20).

3.6 Effects of Suppressive ODN on CD133 Frequency of HepG2 and HepG2-2215

Suppressive ODN (A151) is known to suppress the DNA-driven immunostilmulation and it has been already studied in inflammation related oncogenesis. Since inflammation and cancer growth is closely related, role of inflammation in cancer stem cells is a very important question. Also, another ongoing study showed that suppressive ODN can repress fibrosis which is generally an important step in hepatocarcinogenesis and it also decreases stemness (Aydin, M. et al., unpublished data). To address this, both HepG2 and HepG2-2215 cell lines were treated for one day with high dose (3µM) and low dose (0.5µM) A151, suppressive ODN, and as a control D35 flip was used which does not promote any immune stimulatory or inhibitory effect (Fig. 3.21 & 3.22).
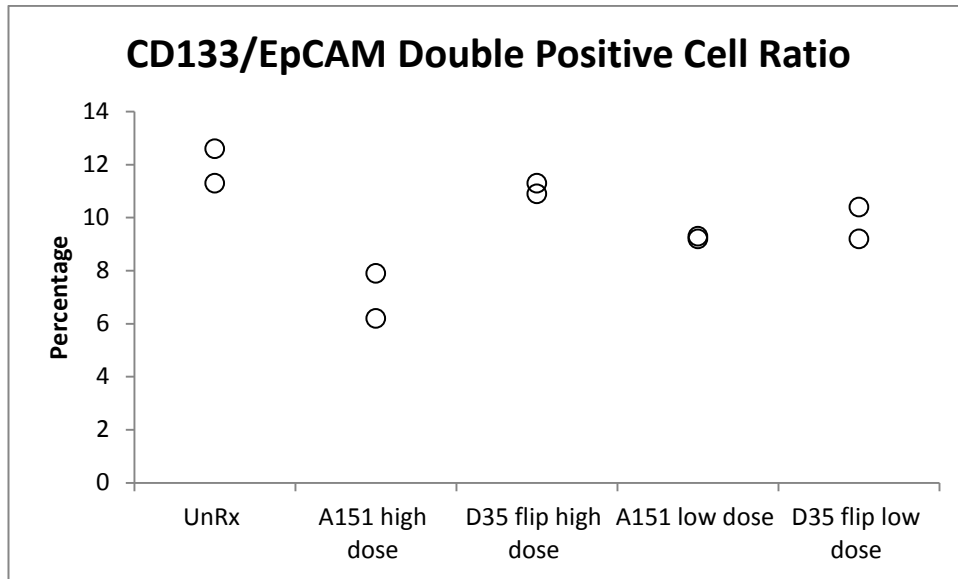
Figure 3.21: *Effects of suppressive ODN (A151) on CD133/EpCAM levels in HepG2.*
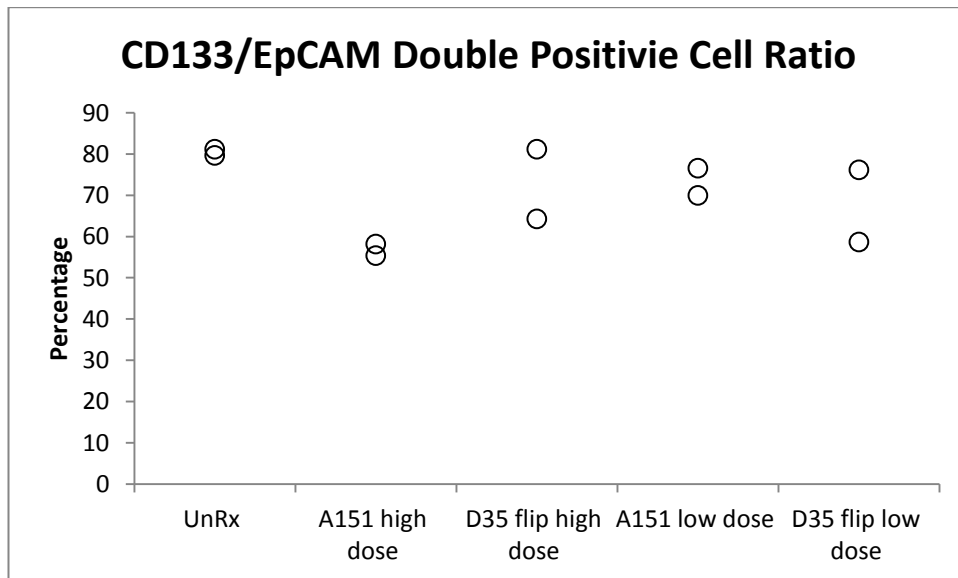
Figure 3.22: *Effects of suppressive ODN (A151) on CD133/EpCAM levels in HepG2-2215.*

These findings suggested that in both HepG2 and HepG2-2215, suppressive ODN treatment decreased CD133/EPCAM levels. However, this one day treatment should be further investigated with longer exposure time and replenishment every day.

Since, suppressive ODN repress DNA-driven immunostimulaton and HepG2-2215 is a cell line that can produce HBV particles because it was transfected with four tandem copies of HBV, these findings suggested that the role of HBV infection should be further investigated to reveal the relationship between HBV and CSC formation. The differential levels of CD133/EpCAM positivity between HEpG2 and HepG2-2215 might be explained via HBV transfection.

CHAPTER 4

DISCUSSION

This study primarily focused on the identification of cancer stem cell populations in HCC-derived cell lines. Using a putative CSC marker in HCC, CD133, these subpopulations were investigated under the effects of different signaling pathways. Also, focus on two cell lines, one parental and one HBV-infected daughter cell line, possible explanations for the increase in CD133$^+$ cell number, were studied

4.1. Identification of Cancer Stem Cells in HCC-derived Cell Lines

After it was shown that many solid tumors, including HCC have cancer stem cells in their tumor bulk that can initiate and maintain the tumor tissue, for the treatment of tumors, targeting CSCs was drawn into the attention [71] To target CSCs, the first aim was to identify and characterize these cells. In HCC, there were many markers to identify CSCs which were associated with either tumorigenicity, or self-renewal, or multipotency [36]. Some of these markers were CD90, CD133, EpCAM, CD44, CD24, CD13, OV6 and so on. However, from all these possible markers, CD90, CD133 and EpCAM were highlighted ones for CSC identification in HCC [34].

Thus, first we aimed to do an initial screen in the panel of 15 HCC-derived cell lines with CD133 to find the frequencies of each cell line's CD133 positivity. Previous studies have shown that different human liver cell lines have different frequencies of CD133$^+$ cells and these cells posses a greater colony forming efficiency and higher proliferation rate along with greater ability to form tumor in vivo [37]. From this initial screen, we found 6 out of 17 cell lines have CD133$^+$ cells as subpopulation. Their CD133 positivity frequencies were changing from 8% to 98% as expected

from previous studies. The next step was to examine effects of different signaling pathways on CSC populations.

4.2 Effects of Wnt Signaling Pathway on CD133^{+} Cell Population

Wnt/β-catenin signaling pathway is a highly conserved pathway that plays a crucial role in embryonic development, growth, survival, regeneration and self-renewal [48]. Apart from these roles, this pathway is associated with hepatic fate specification, prenatal liver development, and liver organogenesis [43]. Finally, it is known that in one third HCC patients, aberrant Wnt activation is observed [46]. These numerous factors led us to investigate possible role of Wnt/β-catenin signaling pathway in CSC regulation. For this initial experiment, we chose a cell line with moderate CD133 positivity, Huh7. This cell line was also broadly used for cancer stem cell studies. Huh7 cells were treated with Wnt/β-catenin pathway activator, Wnt3a, and inhibitor, WIF-1 in order to examine any increase or decrease in the frequency of CD133 positivity. From our findings, CD133+ cells ratio in Huh7 cell line did not change with WIF-1 treatment. Moreover, activation of Wnt/β-catenin signaling pathway via Wnt3a treatment decreased this ratio significantly.

Unfortunately, previous data suggested that elevated levels of Wnt and its downstream mediators were found in CD133^{+} HCC cells [41]. Also, it has been shown that Wnt/β-catenin signaling is associated with activation of tumorigenic liver progenitor cells [72]. However, these studies showed different aspects of link between Wnt/β-catenin signaling and CSCs. First of all, we didn't check for the basal Wnt levels which might be too high that it was saturated. This can explain why further activation of Wnt had negative effects on CD133^{+} cell numbers. On the other hand, WIF-1 is Wnt inhibitory factor 1 which binds to Wnt ligands to prevent their bindings to Frizzled and LRP5/6. Thus, any constitutively active Wnt pathway cannot be inhibited via this way. That might explain why WIF-1 didn't change CD133 levels. Moreover, even though it is known that Wnt/β-catenin pathway is associated with activation of tumorigenic liver progenitor cells, this effect was never

studied on CD133$^+$ cells. So, for Huh7 cell line, Wnt/β-catenin signaling pathway activation may have reverse effects on CD133 positivity which leads to decrease in positivity rate.

4.3 Effects of TGF-β Signaling Pathway on CD133$^+$ Cell Population

TGF-β signaling pathway is a complex pathway that consists of many members and regulates many cellular functions [49]. This signaling pathway has a crucial role in cell cycle regulation, immune system, apoptosis, and embryonic development and so on. TGF-β signaling pathway has a rather complex role during HCC development. Initially, at an early stage of HCC, TGF-β pathway inhibits oncogenesis via inducing apoptosis, and in some HCCs, it has been shown to suppress tumor formation with autophagy activation [47]. However, dysregulated TGF-β signaling is associated with hepatocarcinogenesis [51].

Meanwhile in our initial screen of 17 HCC-derived cell lines, two cell lines came forward because of their high CD133$^+$ cell ratio. This cell line is Hep3B and it has 90% frequency for CD133 positivity. On important fact about this HCC-derived cell line is that this parental cell line was treated with TGF-β1 in stepwise manner to generate a cell line which is TGF-β-resistant. This daughter cell line is Hep3B-TR with more than 90% CD133 positivity.

These facts pointed out that investigation of effects of TGF-β signaling pathway on CD133$^+$ cells in Hep3B might be a perfect candidate to move on. We used Hep3B-TR cell line as a negative control since it is resistant to TGF-β. To activate TGF-β signaling, TGF-β1 was used while inhibition was achieved through anti-TGF-β1 treatment. As a result, it was found out that inhibition of TGF-b signaling did not change CD133$^+$ cell ratio while activation of TGF-b decreased this ratio in Hep3B cell line. And as expected, Hep3B-TR cell line was not affected from both of these treatments.

This might be an expected results overall, when the dual role of TGF-β was considered in HCC. Also, it has been shown that lack of responsiveness to TGF-β led to the generation of CSCs [41]. This result also supports the hypothesis that the interrupted TGF-β signaling pathways might result in HCC because of disruption of a normal pattern of cellular differentiation by hepatic progenitor/stem cells [73, 74]. On the other hand, this result conflicts with a previous study that claims TGF-β is capable of up-regulating CD133 expression in Huh7 cell line in a time- and dose-dependent manner [75]. However, because this study was performed with Huh7 cell line, it is very normal to obtain different results from a different HCC-derived cell line.

4.4 Studies on HepG2 and HepG2-2215 Cell Lines

After these findings, two isogenic cell lines with differential CD133 levels were investigated .Parental HepG2 cell line has the lowest CD133 positivity rate, around 10%, while its clone that is transfected with hepatitis B virus, namely HepG2-2215 has 70-90% CD133$^+$ cell population. Normally, HepG2 is HCC-derived cell line from 15-year-old male, and HepG-2215 is transfected with four 5'-3' tandem copies of the hepatitis B virus (HBV) genome, and can express Hepatitis B e antigen and Hepatitis B surface antigen. Initial results showed that parental HepG2 cell line has around 10-20% CD133$^+$ cells while its clone HepG2-2215 has 70-90% CD133$^+$ cells. Because using single marker for CSC identification is insufficient, we decided to include another marker in our studies to identify CSCs in a more accurate way. This second marker was EpCAM that is associated with invasiveness, self-renewal and tumor formation, and it is widely used in CSC studies in HCC [36]. Then, these two cell lines were analyzed with flow cytometry for double staining of CD133 and EpCAM. As expected, while HepG2 has around 15% double positive cells, HepG2-2215 cell line has more than 75% double positive cells which supports that HepG2-2215 cell line has a higher ratio of cancer stem cells in its population.

One important point we did throughout the experiments was to use serum starvation model to generate harsh conditions where tumor cells will die while cancer stem cells will endure the conditions and thus, their subpopulation will enhance. To test if this hypothesis is true or not, experiments comparing serum free medium treated and untreated HepG2 and HepG2-2215 cell lines were analyzed. The first analysis was performed with CD133 staining. And it reveals that serum starvation model did not affect CD133$^+$ cell frequency in HepG2-2215 cell line. However, the CD133$^+$ cell frequency in HepG2 dropped from 20-25% to 10-15%. This might be explained by the notion that not all CD133 positive cells are cancer stem cells. Thus, only true cancer stem cells kept their status during serum starvation model and the other tumor cells that are CD133 positive died during the treatment in HepG2 cell line. To test this, double staining for EpCAM and CD133 was performed in these two cell lines. We observed a decrease in both HepG2 and HepG2-2215 cell lines. Double positivity frequency decreased from around 90% to 80-75% in HepG2-2215 cell line whereas the decrease in HepG2 was more significantly, dropping from around 10-15% to 2-3%. This might support the idea of not all labeled cells were true CSCs or these results might be the indicator of serum starvation model was not the best idea to enhance CSC population since it affected all the cells without discriminating CSCs from tumor cells.

After these studies, the reason underlying the difference of these two cell lines in the number cancer stem cell population was studied. Firstly, to eliminate any soluble factors, which may cause this CSC population difference, these cell lines were treated with their own media as well as each other's. The results showed that treatment of HepG2 with HepG2 or HepG2-2215 medium did not affect CD133$^+$ cell number and HepG2-2215 was not affected by these treatments as well.

After we could not find any soluble factors that might affect CD133 positivity in these two cell lines, a recent finding caught our attention. It has been shown that activation of Notch dependent cascade or an injury that provokes biliary response causes hepatocytes to go under cellular reprogramming to become an oval cell which will give rise to biliary epithelial cells [68]. In this article, HNF4α was used as hepatocyte marker while Sox9 as biliary epithelial cell marker. Transition from hepatocytes to oval cells and then, to biliary epithelial cells were demonstrated with

double staining of cells with these two markers and cells expressing both of these markers were counted as oval cells that have multipotency to give rise to both hepatocytes and biliary epithelial cells [69]. From this starting point, these markers were used to identify oval cell in these cell lines to assess stemness. Initial data showed that HepG2 has higher levels of HNF4α and Sox9 and these levels decrease upon serum starvation treatment. However, double staining of these cell lines showed that HepG2-2215 has more double positive cells than HepG2, which supports that HepG2-2215 has a stemness-rich nature with a higher CSC population.

All these data, up to this point, supported that HepG2-2215 cell line has more cells with cancer stem cell's features. Since, cancer stem cells are associated with tumor initiation and growth, testing the tumorigenicity potential of these two cell lines was the next step [41]. As expected, HepG2-2215 cell line showed a higher tumor formation and growth rate than HepG2 cell line. After tumorigenicity assay, excised tumor tissues were further investigated for CD133 and EpCAM staining. These data showed that HepG2-2215 has higher CD133$^+$ cell ratio than HepG2, even though cells were injected to a mice and then, single cells were harbored from excised tissue. This was same for the double positive cell numbers as well. So, this analysis showed that HepG2-2215 has higher tumorigenicity potential and after the tumor formation, tumor tissue from HepG2-2215 still has higher number of CD133 and EpCAM positive cells.

4.5 Microarray Study between HeppG2 and HepG2-2215 Cell Lines

To reveal the underlying reasons for the difference in CSC number of these cell lines, a microarray analysis were performed for HepG2 and HepG2-2215 cell lines. Analysis of microarray gave us too many genes and signaling pathways, which these genes are associated with. However, FGFR signaling pathway caught our attention because of many members of this signaling pathway was found to be differentially expressed in these two cell lines. Thus, firstly, FGFR levels of these cell lines were studied. Even though, with serum starvation, FGFR levels dropped, still, HepG2 has significantly higher levels of FGFR than HepG2-2215. These findings suggested that

there might be a inverse proportion between FGFR levels and CSC formation. Thus, activation of FGFR signaling pathway may alter CD133 and EpCAM positive cell numbers in these cell lines. This hypothesis is also supported by the study which showed that reduction in FGFR2IIIb isoform was associated with more aggressive growth of HCC [55]. The aggressiveness of a tumor might be explained by CSC-richness which also supports the reverse relationship between CSCs and FGFR signaling pathway.

Investigation of FGFR signaling via SU5402, which is a potent FGFR inhibitor or siRNA knockdown of FGFR2 were performed to observe the relationship between FGFR levels and CD133/EpCAM positive cell ratios. Initial trials of SU5402 treatment experiments showed a decrease in FGFR2 levels in a dose-dependent manner in both HepG2 and HepG2-2215. However, changes in CD133/EpCAM levels showed no consistency in dose dependent-manner in HepG2-2215 cell line. This might be caused because of very low, basal FGFR levels in HepG2-2215. Meanwhile CD133/EpCAM levels in HepG2 showed a decrease upon SU5402 treatment which was contrary to our hypothesis, surprisingly.

In siRNA treatments, HepG2 cell lines showed a decrease in FGFR levels in dose dependent-manner and luckily, there was a slight increase in its CD133/EpCAM levels, which is not significant. On the other hand, HepG2-2215 showed inconsistent results in both FGFR and CD133/EpCAM levels which remained unexplained. Unfortunately, because of limited time, these experiments could not be repeated. So, the relationship between FGFR signaling and CSCs should be further studied.

Finally, in cancer progression, immune system plays a crucial role. And suppressive ODN (A151), which has been already known with its suppressive role in immunostimulation, was studied in cancer types because of its anti-inflammatory effects. A recent data showed that suppressive ODN can repress fibrosis which is generally previous step of HCC and also down-regulates stem cells (Aydin, M. et al., unpublished data). To test if suppressive ODN, A151, has negative effects on CSC population, HepG2 and HepG2-2215 cell lines were treat with A151. Results showed that A151 decreased the CD133/EpCAM double positive ratio in both HepG2 and HepG2-2215 cells. These exciting results pointed out that the close relationship

between immunity and cancer progression. However, these findings should be further investigated for longer durations and daily replenishments of ODNs for more accurate data.

CHAPTER 5

FUTURE PERSPECTIVES

Microarray analysis between HepG2 and HepG2-2215 cell lines revealed that FGFR signaling might play a role in HCC CSC formation. Experiments targeting FGFR signaling should be repeated for optimization. Optimal doses for both SU5402 to inhibit FGFR pathway and siRNA to knockdown FGFR2 should be found. To confirm these doses, Western blot analysis along with flow cytometry for FGFR2 could be performed. Beside from inhibition, effects of activated FGFR pathway should be investigated via FGFR signaling pathway ligand.

Since, suppressive ODN showed a decrease in CD133/EpCAM positive cell ratios, effects of A151 should be further investigated by administrating the suppressive ODN to cells with longer exposure and daily replenishment. If decrease in the ratios persists, then, more immune-related aspects of hepatocarcinogenesis could be studied to find the effects of immune system on CSCs.

One important aspect of CSCs is that they are chemo- and radio-resistant. To test this, both of these cell lines should be injected to atymic nude mice, again. However, this time, when tumors reached a certain volume, an effective treatment for cancer should be applied to mice in order to see the resistance of these cell lines. Even, HepG2-2215 showed higher tumor formation ability, it is also important that it should also show resistance to treatments. If this cell line is also resistant, then, further studies to find underlying mechanisms of CSCs in HCC can be studied. Moreover, tumorigenicity assay should be repeated with more animals. This time, each cell should be injected to independent animals to avoid any effects that may arise from injecting both cell lines to the same animal. Also, different cell numbers should be injected to mice to see the lowest cell amount to be injected to generate a tumor. Tumorigenicity assay should be performed for a longer duration.

Also, in the case of finding a specific signaling pathway or elements that might be responsible from CSC formation in HCC, such as FGFR pathway or A151, effects of this pathway or these elements should be studied with tumorigenicity assay, and then, the treatment of formed tumors. With this in vivo approach, it can be examined that if found pathway or elements were really linked to CSCs or not. Also, this pathway or these elements may affect only tumor growth or resistance to treatment which will suggest new treatment ways.

Finally, this work was performed on the cell lines rather than primary cell cultures. When it is considered, it is obvious that cell lines were passaged too many times, and they were studied for many years which may cause differentiation of these cell lines. Thus, the results of this study may not represent the reality in normal tumor microenvironment. To reveal more realistic results, after finding a significant result, these experiments should be studied on primary tumor cell lines. Or, fresh tissues directly taken from patients can be investigated.

To sum up, in HCC, formation of CSCs is still unknown and more studies should be done to find the therapeutic approaches to target them or to prevent their formation in the first place.

REFERENCES

[1]   Tat Fan, S. (2010). Liver functional reverse estimation: state of the art and relevance for local treatments. *J Hepatobiliary Pancreat Sci, 17,* 380-384.

[2]   Farazi, P. A., & DePinho, R., A. (2006). Hepatocellular carcinoma pathogenesis: from genes to environment. *Nature Reviews Cancer, 6(9),* 674-687.

[3]   Kim, H. Y., & Park, J. (2014). Clinical Trials of Combined Molecular Targeted Theraphy and Locoregional Therapy in Hepatocellular Carcinoma: Past, Present, and Future. *Liver Cancer, 3,* 9-17.

[4]   Mossanen, J. C., & Tacke, F. (2013). Role of lymphocytes in liver cancer. *OncoImmunology, 2:11, e26468,* 1-9.

[5]   Gomaa, A. I., Khan, S. A., Toledano, M. B., Waked, I., & Taylor-Robinson, S. D. (2008). Hepatocellular carcinoma: Epidemiology, risk factors and pathogenesis. *World J Gastroenterol, 14(27),* 4300-4308.

[6]   Cavazza, A., Caballeria, L., Floreani, A., Farinati, F., Bruguera, M., Caroli, D., & Pares, A. (2009). Incidence, Risk Factors, and Survival of Hepatocellular Carcinoma in Primary Biliary Cirrhosis: Comparative Analysis from Two Centers. *Hepatology, 50,* 1162-1168.

[7]   Gao, J., Xie, L., Yang, W., Zhang, W., Gao, S., Wang, J., et al. (2012). Risk factors of hepatocellular carcinoma – current status and perspectives. *Asian Pacific J Cancer Prev, 13,* 743-752.

[8]   Liu, C., & Kao, J. (2007). Hepatitis B Virus-related Hepatocellular Carcinoma : Epidemiology and Pathogenic Role of Viral Factors. *J Chin Med Assoc, 70(4),* 141-145.

[9]   Shlomai, A., Jong, Y. P., & Rice, C. M. (2014). Virus associated malignancies: The role of viral hepatitis in hepatocellular carcinoma. *Semin Cancer Biol.*

[10] El-Serag, H. B. (2012). Epidemiology of Viral Hepatitis and Hepatocellular Carcinoma. *Gastroenterology, 142(6),* 1264-1273.

[11] Arzumanyan, A., Reis, H. M. G. P. V., & Feitelson, M. A. (2013). Pathogenic mechanisms in HBV- and HCV-associated hepatocellular carcinoma. *Nature Reviews Cancer, 13,* 123-135.

[12] Brechot, C., Kremsdorf, D., Soussan, P., Dejean, A., Brechot, P. P., & Tiollais, P. (2010). Hepatitis B virus (HBV)-related hepatocellular carcinoma (HCC): Molecular mechanisms and novel paradigms, *Pathologie Biologie, 58,* 278-287.

[13] Ke, P., & Chen, S. S. (2012). Hepatitis C Virus and Cellular Stress Response: Implications to Molecular Pathogenesis of Liver Diseases. *Viruses, 4,* 2251-2290.

[14] Cornella, H., Alsinet, C., & Villanueav A. (2011). Molecular Pathogenesis of Hepatocellular Carcinoma. *Alcohol Clin Exp Res, Vol 35, No 5,* 821-825.

[15] French S. W. (2013). Epigenetic Events in Liver Cancer Resulting from Alcoholic Liver Disease. *Alcohol Res., 35(1),* 57-67.

[16] McKillop, I. H., & Schrum, L. W. (2009). Role of alcohol in liver carcinogenesis. *Semin Liver Dis, 29,* 222-232.

[17] Kew, C. M. (2013). Aflatoxins as a Cause of Hepatocellular Carcinoma. *J Gastrointestin Liver Dis, 22(3),* 305-310.

[18] Mohd-Redzwan, S., Jamaluddin, R., Abd.-Mutalib, M. S., & Ahmad, Z. (2013). A mini review on aflatoxin exposure in Malaysia: past, present, and future. *Front Microbiol, 4:133,* 1-8.

[19] Puisieux, A., Lim, S., Groopman, J., & Ozturk, M. (1991). Selective Targeting of p53 Gene Mutational Hotspots in Human Cancers by Etiologically Defined Carcinogens. *Cancer Res, 51,* 6185-6189.

[20] Davilla, J. A., Morgan, R. O., Shaib, Y., McGlynn, K. A., & El-Serag, H. B. (2005). Diabetes increases the risk of hepatocellular carcinoma in the United States: a population based case control study. *Gut, 54,* 533-539.

[21] Facciorusso, A. (2013). The Influence of Diabetes in the Pathogenesi and the Clinical Course of Hepatocellular Carcinoma: Recent Findings and New Perspectives. *Current Diabetes Reviews, 9,* 382-386.

[22] Kikuchi, L., Oliveira, C. P., & Carrilho, F. J. (2014). Nonalcoholic Fatty Liver Disease and Hepatocellular Carcinoma. *Biomed Res Int., 106247.*

[23] Pietrangelo, A. (2009). Iron in NASH, chronic liver diseases and HCC: How much iron is too much? *Journal of Hepatology, 50,* 249-251.

[24] Parfrey, H., Mahadeva, R., and Lomas, D.A. (2003). Alpha(1)-antitrypsin deficiency, liver disease and emphysema. *Int J Biochem Cell Biol 35,* 1009-1014.

[25] Aravalli, R. N., Cressman, E. N. K., & Steer, C. J. (2013). Cellular and molecular mechanisms of hepatocellular carcinoma: an update. *Arch Toxicol, 87,* 227-247.

[26] Llovet, J. M., & Bruix, J. (2008). Molecular Targeted Therapies in Hepatocellular Carcinoma. *Hepatology, 48(4),* 1312-1327.

[27] Aravalli, R. N., Steer, C. J., & Cressman, E. N. K. (2008). Molecular Mechanisms of Hepatocellular Carcinoma. *Hepatology, 48,* 2047-2063.

[28] Ozen, C., Yildiz, G., Dagcan, A. T., Cevik, D., Ors, A., Keles, U., Topel, H., & Ozturk, M. (2013). Genetics and epigenetics of liver cancer. *New Biotechnology, 30,* 381-384.

[29] Bressac, B., Galvin, K. M., Liang, T. J., Isselbacher, K. J., Wands, J. R., & Ozturk, M. (1990). Abnormal structure and expression of p53 gene in human hepatocellular carcinoma. *Proc. Natl. Acad. Sci., 88,* 1973-1977.

[30] Aguillar-Gallardo, C., & Simon, C. (2013). Cells, Stem Cells, and Cancer Stem Cells. *Semin Reprod Med, 31,* 5-13.

[31] O'Connor, M. L., Xiang, D., Shigdar, S. et al. (2013). Cancer stem cells: A contentious hypothesis now moving forward. *Cancer Letters, 344,* 180-187.

[32] Sotiropoulou, P. A., Christodoulou, M. S., Silvani, A., Herold-Mende, C., & Passarella, D. (2014).Chemical approaches to targetinf drug resistance in cancer stem cells. *Drug Discov Today, 14.*

[33] Yamashita, T., & Wang, X. W. (2013). Cancer stem cells in the development of liver cancer. *J Clin Invest, 123(5),* 1911-1918.

[34]   Ji, J., & Wang, X. W. (2012). Clinical Implications of Cancer Stem Cell Biology in Hepatocellular Carcinoma. *Semin Oncol, 39(4),* 461-472.

[35]   Nagano, H., Ishii, H., Marubashi, S., Haraguchi N., Eguchi, H., Doki, Y., & Mori, M. (2012). Novel therapeutic target for cancer stem cells in hepatocellular carcinoma. *J HepatobilliaryPancreat Sci, 19,* 600-605.

[36]   Wah Lee, T. K., Cheung, V. C. H., & Ng, I. O. L. (2012). Liver tumor-initiating cells as a therapeutic target for hepatocellular carcinoma. *Cancer Letters, 338,* 101-109.

[37]   Tong, C. M., Ma, S., & Guan, X. (2011). Biology of hepatic cancer stem cells. *J Gastroenterol Hepatol 26(8),* 1229-1237.

[38]   Ma, S. (2013). Biology and clinical implications of CD133$^+$ liver cancer stem cells. *Experimental Cell Research, 319,* 126-132.

[39]   Liu, L., Fu, D., Ma, Y., & Shen, X. (2011). The Power and the Promise of Liver Cancer Stem Cell Markers. *Stem Cells and Development, 20(12),* 2023-2030.

[40]   Imrich, S., Hachmeister, M., & Gires, O. (2012). EpCAM and its potential role in tumor-initiating cells. *Cell Adhesion & Migration, 6(1),* 30-38.

[41]   Marquardt, J. U., Factor, V. M., & Thorgeirsson, S. S. (2010). Epigenetic regulation of cancer stem cells in liver cancer: Current concepts and clinical implications. *J Hepatol, 53(3),* 568-577.

[42]   Majumdar, A et al. (2012). Hepatic stem cells and transforming growth factor β in hepatocellular carcinoma. *Nat Rev Gastroenterol Hepatol, 9(9),* 530-538.

[43]   Behari, J. (2010). The Wnt/β-catenin signaling pathway in liver biology and disease. *Expert Rev Gastroenterol Hepatol, 4(6),* 745-756.

[44]   Rosenbluh, J., Wang, X., & Hahn, W. C. (2013). Genomic insights into WNT/β-catenin signaling. *Trends in Pharmacological Sciences, 25(2),* 103-109.

[45]   Dahmani, R., Just, P., & Perret, C. (2011). The Wnt/β-catenin pathway as a therapeutic target in human hepatocellular carcinoma. *Clin Res Hepatol Gastroenterol, 35(11),* 709-713.

[46]   Oishi, N., & Wang, X. W. (2011). Novel therapeutic Strategies for Targeting Liver Cancer Stem Cells. *Int. J. Biol., 7(5),* 517-535.

[47] Sng, K., Wu, J., & Jiang, C. (2013). Dysregulation of signaling pathways and putative biomarkers in liver cancer stem cells. *Oncology Reports, 29,* 3-12.

[48] Yao, Z., & Mishra, L. (2009). Cancer stem cells and hepatocellular carcinoma. *Cancer Biol Ther., 8(18),* 1691-1698.

[49] Zhang, S., Sun, W., Wu, J., & Wei, W. (2014). TGF-β signaling pathway as a pharmacological target in liver diseases. *Pharmacol Res.*

[50] Yamazaki, K., Masugi, Y., & Sakamoto, M. (2011). Molecular Pathogenesi of Hepatocellular Carcinoma: Altering Transforming Growth Factor-β Signaling in Hepatocarcinogenesis. *Dig Dis,29,* 284-288.

[51] Mishra, L. et al. (2009). Liver Stem Cells and Hepatocellular Carcinoma. *Hepatology, 49(1),* 318-329.

[52] Chiba, T., Kamiya, A., Yokosuka, O., & Iwama, A. (2009). Cancer stem cells in hepatocellular carcinoma: recent progress and perspective. *Cancer Letters, 286,* 145-153.

[53] Raju, R. et al. (2014). A Network Map of FGF-1/FGFR Signaling System. *Journal of Signal Transduction, 2014(962962).*

[54] Ahmad, I., Iwata, T., & Leung, H. Y. (2012). Mechanisms of FGFR-mediated carcinogenesis. *Biochimica et Biophysica Acta, 1823*, 850-860.

[55] Amann, T. et al. (2010). Reduced Expression of Fibroblast Growth Factor Receptor 2IIIb in Hepatocellular Carcinoma Induces a More Aggressive Growth. *The American Journal of Pathology, 176(3),* 1433-1442.

[56] Narasu, L. et al. (2013). Fibroblast Growth Factor Receptor Imhibitors. *Curr Parmacol Des, 19,* 687-701.

[57] Dienstmann, R. et al. (2013). Genomic aberrations in the FGFR pathway: opportunities for targeted therapies in solid tumors. *Annals of Oncology, 00,* 1-12.

[58] Gauglhofer, C., Sagmeister, S. etal. (2011). Up-Regulation of the Fibroblast Growth Factor 8 Subfamily in Human Hepatocellular Carcinoma for Cell Survival and Neoangiogenesis. *Hepatology, 53,* 854-864.

[59] Medzhitov, R. (2007). Recognition of microorganisms and activation of the immune response. *Nature, 449,* 819-826.

[60] Ishii, K. J., & Akira, S. (2005) Innate immune recognition of nucleic acids: Beyond toll-like receptors. *Int. J. Cancer, 117,* 517-523.

[61] Ishii, K. J., Gursel, I., Gursel, M., & Klinman, D. M. (2004). Immunotherapeutic utility of stimulatory and suppressive oligodeoxynucleotides. *Curr Opin Mol Ther, 6(2),* 166-74.

[62] Krieg, A. M., Wu, T., Weeratna, R., Efler, S. M., Love-Homan, L., Yang, L., Yi, A., Short, D., & Davis, H. L. (1998). Sequence motifs in adenoviral DNA block immune activation by stimulatory CpG motifs. *Proc. Natl. Acad. Sci., 95,* 12631-12636.

[63] Gursel, I., Gursel, M., Yamada, H., Ishii, K. J., Takeshita, F. & Klinman, D. M. (2003). Repetitive elements in mammalian telomeres suppress bacterial DNA-induced immune activation. *J Immunol, 171(3),* 1393-1400.

[64] Ikeuchi, H., Kinjo, T., & Klinman, D. M. (2011). Effect of suppressive oligodeoxynucleotides on the development of inflammation-induced papillomas. *Cancer Prev Res (Phila), 4(5),* 752-757.

[65] Takahashi, R., Sato, T., Klinman, D. M., Shimosato, T., Kaneko, T., & Ishigatsubo, Y. (2013). Suppressive oligodeoxynucleotides synergistically enhance antiproliferative effects of anticancer drugs in A549 human lung cancer cells. *Int J Oncol, 42(2),* 429-36.

[66] Simon, R., Lam, A., Li, M. C., Ngan, M., Menenzes, S., & Zhao, Y. (2007). Analysis of gene expression data using BRB-Array Tools. *Cancer Inform, 3,* 11-17.

[67] Yuzugullu, H. et al. (2009). Canonical Wnt signaling is antagonized by noncanonical Wnt5a in hepatocellular carcinoma cells. *Mol Cancer, 8:90.*

[68] Yanger, K., Zong, Y., Maggs, L. R. et al. (2013). Robust cellular reprogramming occurs spontaneously during liver regeneration. *Genes Dev, 27,* 719-724.

[69] Fausto, N., & Campell, J. S. (2003). The role of hepatocytes and oval cells in liver regeneration and repopulation. *Mechanisms of Development, 120,* 117-130.

[70] Oh, S., Hatch, H. M., & Peterson, B. E. (2002). Hepatic oval 'stem' cell in liver regeneration. *Semin Cell Dev Biol., 13(6),* 405-409.

[71]   Zheng, Y. et al. (2013). The CD133$^+$CD44$^+$ Precancerous Subpopulation of Oval Cells is a Therapeutic Target for Hepatocellular Carcinoma. *Stem Cells Dev.*

[72]   Yang, W., Yan, H., Chen, L. et al. (2008). Wnt/β-Catenin Signaling Contributes to Activation of Normal and Tumorigenic Liver Progenitor Cells. *Cancer Res, 68,* 4287-4295.

[73]   Amin , R., & Mishra, L. (2008). Liver Stem Cells and TGF-β in Hepatic Carcinogenesis. *Gastrointest Cancer Res, 2(4Suppl),* 27-30.

[74]   Tang, Y., Kitisin, K, et al. (2008). Progenitor/stem cells give rise to liver cancer due to aberrant TGF-β and IL-6 signaling. *Prot Natl Acad Sci USA, 105(7),* 2445-2450.

[75]   You, H., Ding, W., & Rountree, C. B. (2010). Epigenetic Regulation of Cancer Stem Cell Marker CD133 by Transforming Growth Factor-β. *Hepatology, 51,* 1635-1644.

APPENDIX

APPENDIX A

Appendix A1. Negative Effects of Wnt Pathway Activation

Wnt/β-catenin signaling pathway regulates stem cell pluripotency and cell fate decisions during development via cross-talking with other pathways, such as retinoic acid, TGF-β, FGF and BMP [44]. It has been known that this signaling has a role in liver development while aberrant Wnt signaling has also been linked to HCC [43]. Thus, in order to study effects of Wnt signaling on cancer stem cells in HCC, in one of the CD133 positive cell lines, Wnt pathway was activated by its ligand Wnt-3a and inhibited by WIF-1. For this experiment, Huh7 cell line was chosen because of its moderate CD133 positivity (Fig. A1.1). Also, cells were seeded in low density to observe colony formations. In Wnt signaling, the pathway is activated via binding of a Wnt ligand, like Wnt-3a. This reagent was directly added to the medium of the cells as the inhibitor WIF-1, which inhibits the signaling by binding to the ligand and preventing its activation ability.
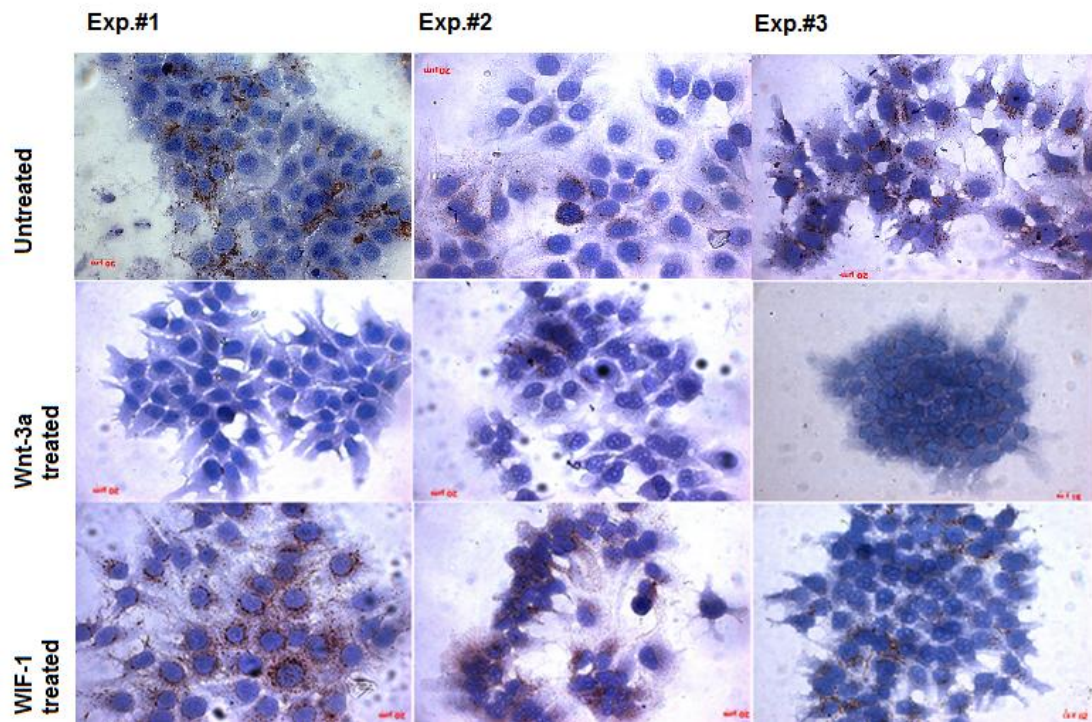
Figure A1.1: *Differential Effect of Wnt-signaling pathway in response to activator or inhibitor treatment on CD133 expression levels of Huh7 via immunoperoxidase procedure. Bright field microscope, 40X.*

After the immunoperoxidase staining, with the help of a bright field microscopy, formed colonies with more than 50 cells were counted and their CD133 positivity assessed as higher than 80%, lower than 20% or in between. Then, these countings were statistically analyzed and Student's t-test was performed (Fig. A1.2). From these staining trials, it has been shown that while WIF-1 treatment did not change CD133 frequency of Huh7 cell line, Wnt-3a treatment showed a decrease in the positivity. And statistical analysis, namely Student's t test confirmed these findings.
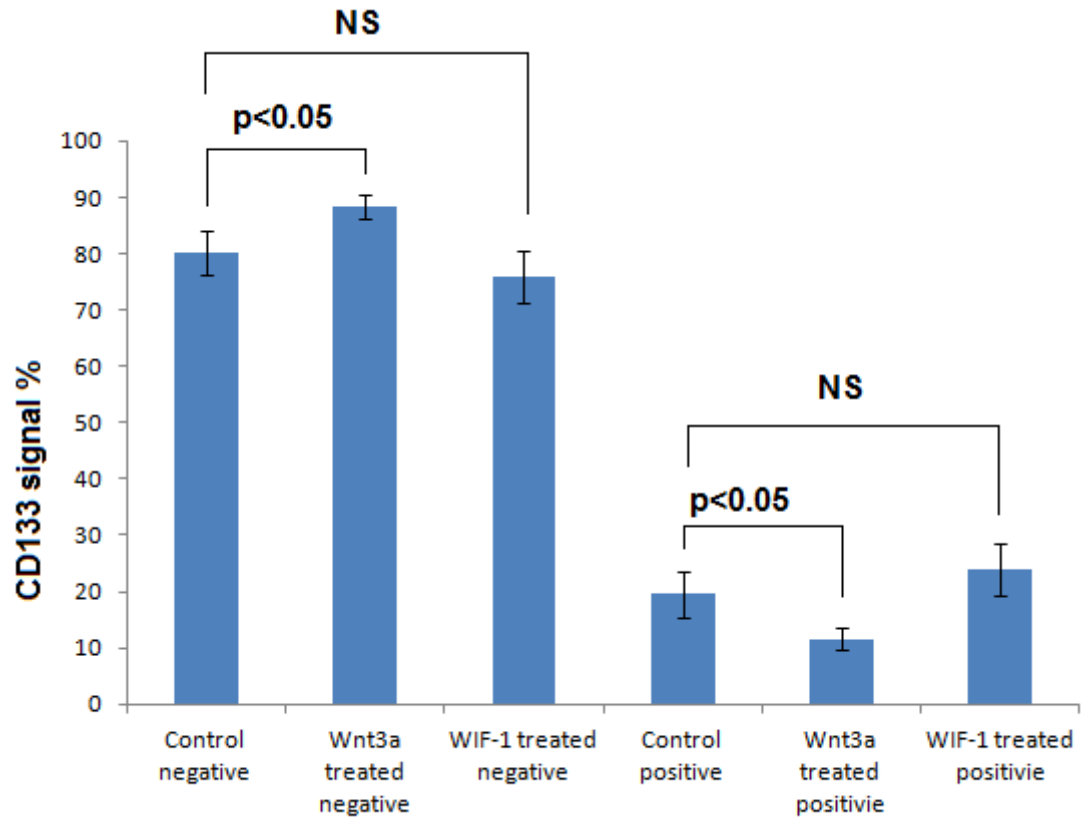
Figure A1.2: *Differential Effect of Wnt-signaling pathway in response to activator or inhibitor treatment on CD133 expression levels of Huh7 (p<0.05, NS=not significant).*

Appendix A2. Negative Effects of TGF-β Pathway Activation

After it has been found that Wnt pathway activation is decreasing the CD133 positivity in Huh7 cell line (Fig. A1.2), other pathways' effects were examined. In the set of 17 HCC-derived cell lines, there were two cell lines with the highest CD133$^+$ ratios. These cell lines were Hep3B, which is epithelial, liver cell line taken from an 8-year-old juvenile, and its isogenic cell line, Hep3B-TR, which is a Hep3B-derived cell line that rendered a resistance to TGF-β by stepwise exposure to TGF-β1. And Hep3B cell line has CD133 positivity frequency between 80- 90%, while Hep3B-TR cell line has more than 90% CD133 positivity. Thus, these two cell lines were a great chance to study the effects of TGF-β signaling pathway that controls proliferation, cellular differentiation and other functions [50]. Another important point about TGF-β is that the activation of this signal cascade is closely related to fibrosis, liver cirrhosis and subsequent HCC development [52].

The effects of TGF-β signaling pathway were examined through the treatment of these cell lines with a TGF-β pathway activator and inhibitor (Fig. A2.3). The activator was TGF-β1 while the inhibitor was anti-TGF-β1 antibody. Because it has been already known that Hep3B-TR is a cell line resistant to TGF-β signaling, the aim of using that cell line was to have a negative control. After the treatment, these two cell lines were analyzed with immunoperoxidase and flow cytometry for CD133 positivity (Figs. A2.3 & A2.4).
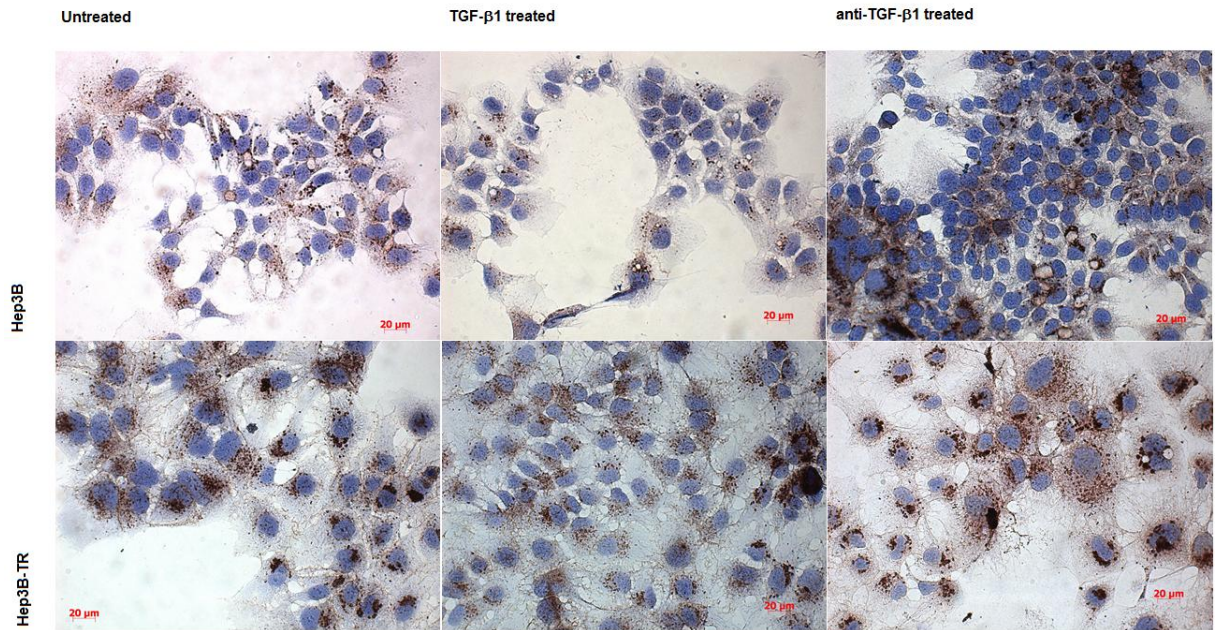
Figure A2.3: *Effects of TGF-β signaling pathway in response to activator and inhibitor on CD133 levels of Hep3B and Hep3B-TR cell lines by immunoperoxidase. Bright field microscopy, 40X.*
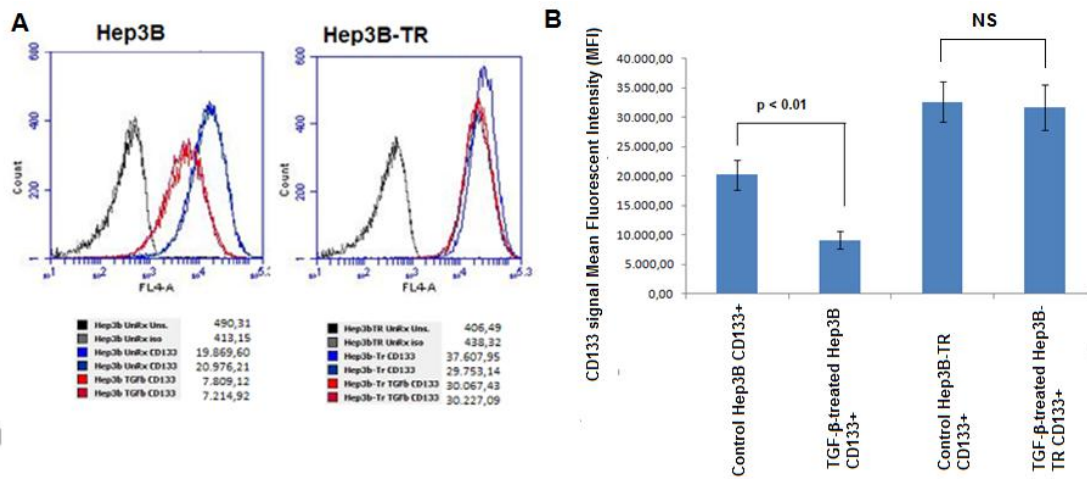

Figure A2.4: *Effects of TGF-b signaling pathway on CD133+ cell frequency in Hep3B and Hep3B-TR cell lines by flow cytometry analysis in panel A. Data was statistically analyzed with Student's t test, p<0.01, panel B.*

These findings showed that activation of TGF-β signaling pathway has negatively affected CD133$^+$ HCC subpopulation in Hep3B cell line. However, inhibition of TGF-b pathway did not affect CSC population. As expected, Hep3B-TR cell line was acted as negative control and didn't show any changes in both treatments that activated and inhibited TGF-β pathway.

Appendix A3. Flow Cytometry Analysis of Xenograft Tumor Tissues
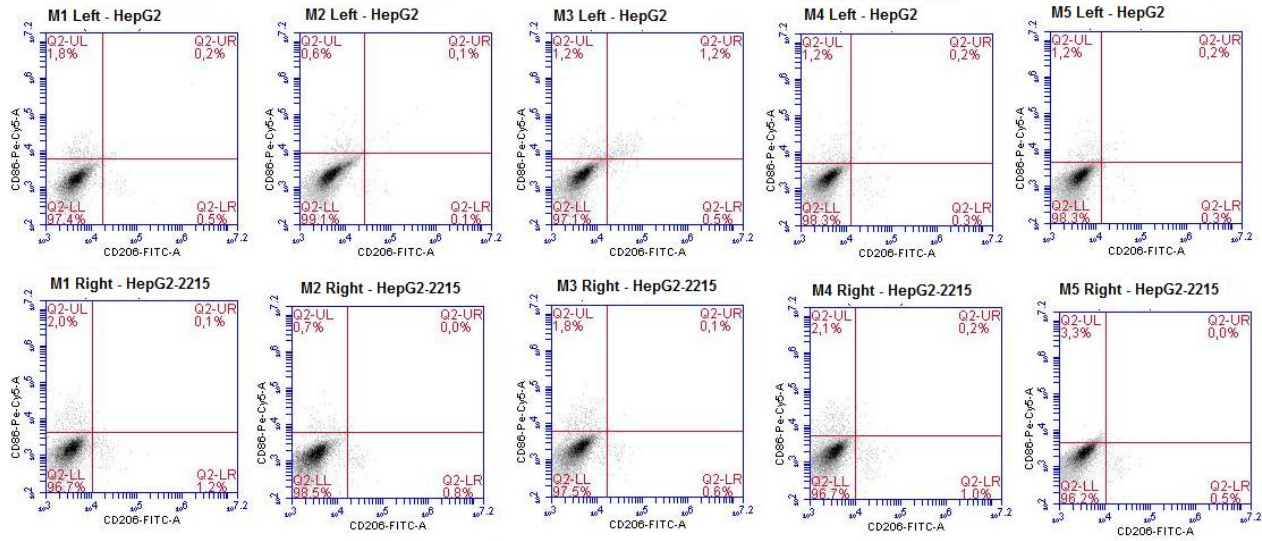
Figure A3.5: *Detection of M1/M2 macrophage levels of HepG2- and HepG2-2215-derived tumor samples by flow cytometry analysis.*

After tumors were taken from nude mice that were injected with HepG2 cells to their left sides and HepG2-2215 to their right sides, these cells were dissociated to obtain single cell suspension. Cells were stained for M1 (CD86 as a marker) and M2 (CD206 as a marker) markers to study tumor microenvironment. However, there was no consistent result and these results showed that in these tumors' microenvironments, M1 and M2 levels were very low.

Appendix A4. Gene Set Enrichment Analysis of Microarray Study

Table A4.1: *Differentially expressed gene sets belonging to development or differentiation category.*

Gene Set	Enriched in sample	Transcription factor
V$HNF4ALPHA_Q6	HepG2	HNF4A
V$HNF6_Q6	HepG2	HNF6A
V$HOXA3_01	HepG2	HOXA3

Table A4.2: *Differentially expressed gene sets belonging to stem cells category.*

Gene Set	Enriched in sample
MIKKELSEN_PLURIPOTENT_STATE_DN	HepG2-2215
ZHOU_PANCREATIC_ENDOCRINE_PROGENITOR	HepG2-2215
RPS14_DN.V1_UP	HepG2-2215
BOQUEST_STEM_CELL_UP	HepG2
HOFMANN_MYELODYSPLASTIC_SYNDROM_LOW_RISK_UP	HepG2
INGRAM_SHH_TARGETS_DN	HepG2
PARK_OSTEOBLAST_DIFFERENTIATION_BY_PHENYLAMIL_UP	HepG2
REACTOME_REGULATION_OF_KIT_SIGNALING	HepG2

Gene Set		Enriched in Sample
BMI1_DN.V1_DN		HepG2
BMI1_DN_MEL18_DN.V1_DN		HepG2

Table A4.3: *Differentially expressed gene sets belonging to signaling pathways category.*

Gene Set	Sub-category	Enriched in Sample
BIOCARTA_INTEGRIN_PATHWAY	Cell-cell junction signaling	HepG2
PID_SYNDECAN_4_PATHWAY	Cell-cell junction signaling	HepG2
PID_NECTIN_PATHWAY	Cell-cell junction signaling	HepG2
PID_EPHA_FWDPATHWAY	Cell-cell junction signaling	HepG2
PID_FAK_PATHWAY	Cell-cell junction signaling	HepG2
PID_AVB3_INTEGRIN_PATHWAY	Cell-cell junction signaling	HepG2
REACTOME_CELL_CELL_JUNCTION_ORGANIZATION	Cell-cell junction signaling	HepG2
REACTOME-CELL_CELL_COMMUNICATION	Cell-cell junction signaling	HepG2
REACTOME_PECAM1_INTERACTIONS	Cell-cell junction signaling	HepG2

REACTOME_ADHERENS_JUNCTIONS_INTERACTIONS	Cell-cell junction signaling	HepG2
REACTOME_DOWNSTREAM_SIGNALING_OF_ACTIVATED_FGFR	FGFR signaling	HepG2
REACTOME_NEGATIVE_REGULATION_OF_FGFR_SIGNALING	FGFR signaling	HepG2
REACTOME_SIGNALING_BY_FGFR	FGFR signaling	HepG2
REACTOME_SIGNALING_BY_FGFR_IN_DISEASE	FGFR signaling	HepG2
REACTOME_FGFR4_LIGAND_BINDING_AND_ACTIVATION	FGFR signaling	HepG2
REACTOME_FRS2_MEDIATED_CASCADE	FGFR signaling	HepG2
KEGG_INSULIN_RECEPTOR_SIGNALLING_PATHWAY	Insulin signaling	HepG2
REACTOME_INSULIN_RECEPTOR_SIGNALING_CASCADE	Insulin signaling	HepG2
REACTOME_SIGNALING_BY_INSULIN_RECEPTOR	Insulin signaling	HepG2
KRAS_DF.V1_UP	Ras signaling	HepG2-2215
KRASKIDNEY_UP.V1_UP	Ras signaling	HepG2-2215
KRAS_SO_UP.V1_UP	Ras signaling	HepG2-2215
KARAKAS_TGFB1_SIGNALING	TGF-beta signaling	HepG2-2215
TGFB_UP.V1_DN	TGF-beta signaling	HepG2

Table A4.4: *Differentially expressed gene sets belonging to viral infection, HCC or cancer category.*

Gene Set	Enriched in sample
PHONG_TNF_TARGETS_UP	HepG2-2215
V$AP4_Q5	HepG2-2215
V$AP4_Q6_01	HepG2-2215
V$EFC_Q6	HepG2-2215
V$ICSBP_Q6	HepG2-2215
V$IRF_Q6	HepG2-2215
TTAYRTAA_V$E4BP4_01	HepG2-2215
CERVERA_SDHB_TARGETS_2	HepG2
SHETH_LIVER_CANCER_VS_TXNIP_LOSS_PAM1	HepG2
V$CEBPGAMMA_Q6	HepG2
V$RFX1_02	HepG2

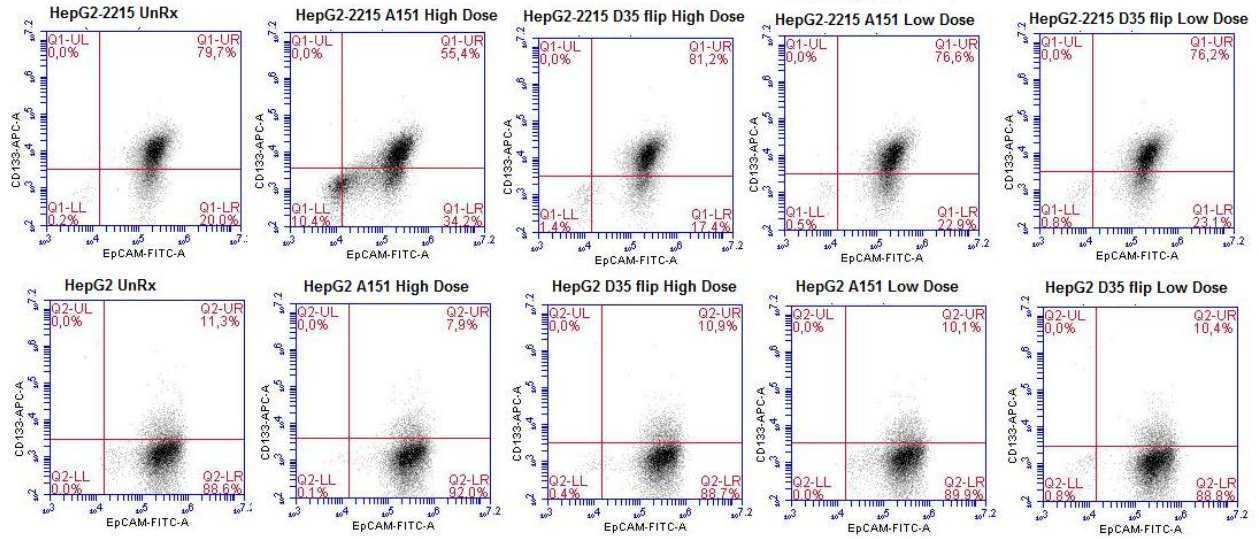## Appendix A5. Effects of Suppressive ODN Treatment on CD133 Levels

***Figure* A5.6:** *Effects of suppressive ODN (A151) treatment on CD133/EpCAM levels of HepG2 and HepG2-2215 cell lines by flow cytometry analysis.*